

2018

## **Plants as Biofactories to Produce Mammalian Tumor Suppressor Micornas**

John Lachlan MacArthur  
*University of South Carolina*

Follow this and additional works at: <https://scholarcommons.sc.edu/etd>



Part of the [Biological Engineering Commons](#)

---

### **Recommended Citation**

MacArthur, J.(2018). *Plants as Biofactories to Produce Mammalian Tumor Suppressor Micornas*. (Doctoral dissertation). Retrieved from <https://scholarcommons.sc.edu/etd/4504>

This Open Access Dissertation is brought to you by Scholar Commons. It has been accepted for inclusion in Theses and Dissertations by an authorized administrator of Scholar Commons. For more information, please contact [digres@mailbox.sc.edu](mailto:digres@mailbox.sc.edu).

PLANTS AS BIOFACTORIES TO PRODUCE MAMMALIAN TUMOR SUPPRESSOR  
MICRORNAS

by

John Lachlan MacArthur

Bachelor of Science  
University of South Carolina, 2012

---

Submitted in Partial Fulfillment of the Requirements

For the Degree of Doctor of Philosophy in

Biological Sciences

College of Arts and Sciences

University of South Carolina

2018

Accepted by:

Vicki S. Vance, Major Professor

Lewis H. Bowman, Chair, Examining Committee

Beth Krizek, Committee Member

Maria Marjorette O. Peña, Committee Member

Lorne J. Hofseth, Committee Member

Cheryl L. Addy, Vice Provost and Dean of the Graduate School

© Copyright by John Lachlan MacArthur, 2018  
All Rights Reserved.

## DEDICATION

This work is dedicated to my beautiful wife Matilda. Without her love, support, and strength I would not be the man I am today. She will always be the driving force behind everything I do. This work is also dedicated to my friend Christopher Esckelson, who passed onto the next life too early in service of this great country. He is responsible for setting me on my course of enlightenment, without him I may have never had the courage to pursue a higher education.

## ACKNOWLEDGEMENTS

I would like to acknowledge my mentor Dr. Vicki Vance and also my fellow lab member Dr. Gail Pruss. They are brilliant scientists that have helped develop my critical thinking, scientific reasoning, and writing skills. I would like to thank former fellow lab members Dr. Amy Wahba, Dr. Matt Endres, and Dr. Sizo Mlotsha, who have been instrumental in my success by providing technical, academic, and often emotional support. I would like to acknowledge the members of my committee, Dr. Lewis Bowman, Dr. Beth Krizek, Dr. Maria Marjorette O. Peña, and Dr. Lorne J. Hofseth for their guidance and support throughout my graduate student career. I would especially like to thank fellow graduate students Ellen Richardson, Dr. Heather Mentrup, Dr. Timothy Hines, and Hossam Tashkandi for being great friends and providing support throughout graduate school. Thank you to all the friends I have made over the years while in South Carolina, they have all become like family to me and I appreciate having them in my life. I would like to thank the Eस्कелsons and my father and mother-in-law, Dave and Patti, for all the support they have provided Matilda and I over the years. To my parents, Ben and Vicki, thank you for teaching me to have a strong and unwavering drive to succeed. They have supported me in everything I've ever done, and for that I am forever grateful. A big thank you goes to my siblings Tony, Ben, and Stephanie. They have been a source of inspiration and strength for my entire life and I admire them dearly, we are the invincible MacArthurs.

## ABSTRACT

MicroRNAs (miRNAs) are small noncoding single stranded RNAs that are considered master regulators of gene expression. They are also an emerging class of therapeutic agents with significant potential for the prevention and treatment of many diseases, including cancer. Many different forms of cancer are associated with loss or reduced accumulation of one or more miRNAs that function as tumor suppressors. In animal models, restoration of missing tumor suppressor miRNAs prevents the initiation, progression and/or spread of the disease. However, the current absence of an efficient method for delivery of therapeutic miRNAs is a critical barrier to their use. The research in this thesis has tested a novel chemopreventive strategy for miRNA replacement therapy based on ingestion of plant matter that has been bioengineered to produce mammalian tumor suppressor miRNAs. The work builds on the Vance lab's promising pilot study showing that oral administration of plant RNA spiked with a cocktail of three tumor-suppressor miRNAs (miR-34a, -143, and -145), synthesized with the 3'-methylation characteristic of plant miRNAs, has significant chemopreventive activity in the *Apc<sup>Min/+</sup>* mouse, a well-established animal model of colon cancer. Based on this work, *Arabidopsis thaliana* was bioengineered to produce the same three tumor suppressor miRNAs used in the earlier study. This required devising strategies to engineer miRNAs that are not the standard 21 nt size of most plant miRNAs. In a small pilot study using these

plant-made tumor suppressor miRNAs, we found that *Apc<sup>Min/+</sup>* mice that were fed a diet containing the transgenic Arabidopsis tissue developed significantly fewer tumors than mice fed a control diet that was calorically and nutritionally matched, but did not contain plant tissue. Although the results using this delivery method were promising, the approach was limited experimentally due to the low concentration of the miRNAs in lyophilized tissues as well as the feeding preferences of the mice. Thus, subsequent work focused on a strategy to deliver high levels of plant-made miRNAs by packaging them into plant exosome-like vesicles, which are taken up by the mammalian digestive tract after ingestion. For plant exosome-like vesicles to be effective in future studies, techniques for enhancing the loading of bioengineered miRNAs were developed. Work reported here points to the importance of the identity of the 5' nucleotide of the engineered miRNA for efficient loading into plant exosome-like vesicles for subsequent delivery by ingestion.

## TABLE OF CONTENTS

DEDICATION.....	iii
ACKNOWLEDGEMENTS .....	iv
ABSTRACT .....	v
LIST OF FIGURES.....	ix
LIST OF TABLES.....	xi
LIST OF ABBREVIATIONS.....	xii
CHAPTER 1: INTRODUCTION .....	1
1.1 MICRORNAS.....	1
1.2 ROLE OF MIRNA DYSREGULATION IN DISEASE .....	1
1.3 CROSS KINGDOM GENE REGULATION BETWEEN PLANTS AND ANIMALS .....	2
1.4 PLANTS TO PRODUCE AND DELIVERY TUMOR SUPPRESSOR MIRNAS .....	3
CHAPTER 2: DESIGN OF MIRNA CONSTRUCTS AND GENERATION OF TRANSGENIC LINES.....	4
2.1 INTRODUCTION.....	4
2.2 RESULTS AND DISCUSSION .....	6
CHAPTER 3: FEEDING EXPERIMENT: DIETARY DELIVERY OF MAMMALIAN TUMOR SUPPRESSOR MIRNAS .....	15
3.1 INTRODUCTION.....	15
3.2 RESULTS AND DISCUSSION .....	18
CHAPTER 4: PLANT EXOSOME-LIKE VESICLES: A POTENTIAL DELIVERY VEHICLE FOR MIRNAS .....	37

4.1 INTRODUCTION.....	37
4.2 RESULTS AND DISCUSSION .....	39
CHAPTER 5: MATERIALS AND METHODS .....	50
REFERENCES.....	59

## LIST OF FIGURES

Figure 2.1 miRNA/miRNA* region of miRNA constructs .....	11
Figure 2.2 miRNA/miRNA* region of 23nt miRNA constructs .....	12
Figure 2.3 Production of three mouse miRNAs in bioengineered plants.....	13
Figure 2.4 miRNA isomiR distributions in bioengineered plants. ....	14
Figure 3.1 Images of fresh, juiced, and lyophilized Arabidopsis .....	25
Figure 3.2 miR-143 stability in juice .....	26
Figure 3.3 miR-143 and miR-34a stability in lyophilized plant tissue .....	27
Figure 3.4 Stability of endogenous plant miR159a during simulated mouse chow incorporation .....	28
Figure 3.5 Stability of miR-143 incorporated in 10% <i>Arabidopsis</i> diet.....	29
Figure 3.6 Average weight of <i>Apc<sup>Min/+</sup></i> mice and average weights of diets consumed .....	30
Figure 3.7 Average <i>Apc<sup>Min/+</sup></i> mice tumor burden in mice consuming 10% miR or purified diets. ....	31
Figure 3.8 Fold change of miRNAs and miRNA targets in mice fed miR and purified diets .....	32
Figure 3.9 Fold change of miRNA targets in mice fed miR and purified diets .....	33
Figure 4.1 Levels of miRNAs loaded into EVs .....	44
Figure 4.2 Image of EVs .....	45

Figure 4.3 miR-143 localization in floating and non-floating EV prep.....	46
Figure 4.4 Stability of miR-143 in EVs after lyophilization .....	47
Figure 4.5 Alternative size and starting nucleotide constructs of miR-145.....	48
Figure 4.6 Levels of miR-145 constructs loaded into EVs.....	49

## LIST OF TABLES

Table 3.1 Nutritional and caloric values of lyophilized <i>Arabidopsis</i> .....	34
Table 3.2 Nutritional components added to miR and purified diets .....	35
Table 3.3 Final nutritional content of miR and purified diets. ....	36

## LIST OF ABBREVIATIONS

Apc.....	<i>adenomatous polyposis coli</i>
CRC .....	Colorectal Cancer
DCL1.....	Dicer-like 1
EVs .....	exosome-like vesicles
Min .....	multiple intestinal neoplasia
miRNA .....	microRNA
miR159a .....	microRNA159a
miR319a .....	microRNA319a
miR-34a .....	microRNA-34a
miR-143 .....	microRNA-143
miR-145 .....	microRNA-145
mRNA .....	messenger RNA
RISC .....	RNA-induced silencing complex

# CHAPTER 1

## INTRODUCTION

### 1.1 MICRORNAS

microRNAs (miRNAs) are small noncoding single stranded RNAs that are considered master regulators of gene expression (Carthew, Richard W. and Sontheimer 2009). These small noncoding RNAs are a highly conserved part of an ancient pathway of gene regulation that exists in nearly all eukaryotic organisms (Cai et al. 2009). They incorporate into a protein complex called the RNA-induced silencing complex (RISC), in which the miRNA acts as a guide to target specific messenger RNAs (mRNAs) using the base pairing rules (Schanen and Li 2011). Once RISC and its attached miRNA are bound to a target mRNA, translation is blocked either directly or by mRNA degradation (Fabian et al. 2009). Because a single miRNA can potentially have hundreds of targets, this method of gene regulation is both complex and highly versatile (Graves and Zeng 2012).

### 1.2 ROLE OF MIRNA DYSREGULATION IN DISEASE

MiRNAs control many cellular processes, ranging from metabolism to cellular proliferation and differentiation. When the normal balance of miRNAs is disrupted, it can lead to a wide variety of human diseases, including many forms of cancer (Jansson and Lund 2012). Because miRNAs are both highly specific

and effective gene regulators, their potential as therapeutic agents is now widely recognized (van Rooij and Kauppinen 2014). It has been shown in both animal models and tissue culture cells that if therapeutic miRNAs can be introduced to diseased tissue, many diseases can be inhibited, blocked, or even regressed (Bader, Brown, and Winkler 2010). Although miRNAs are a promising therapeutic agent, development of methods to deliver small RNAs is a challenging problem that has been the focus of much research (Hellman and Fried 2009). Current strategies involve chemically altering miRNAs or using nanoparticles to increase both stability and uptake (Bader et al. 2011). These delivery techniques are not only expensive, they may also introduce toxicity and reduce the effectiveness of the miRNAs.

### 1.3 CROSS KINGDOM GENE REGULATION BETWEEN PLANTS AND ANIMALS

Recently, the existence of cross kingdom gene regulation between plants and animals via ingestion of plant tissues was reported (Zhang et al., 2012). This discovery was made when endogenous plant miRNAs were found in mammals and shown to be functional to regulate expression of mammalian genes (Zhang et al., 2012). This ground-breaking publication presented evidence that endogenous plant miR168a, an abundant rice miRNA, was absorbed by the mammalian GI tract. The only possible source of this plant miRNA was from the animal's diet. miR168a was found in several tissues, including the heart, spleen, lung, kidney, stomach, small intestine, and brain, and it was found to target low-density lipoprotein receptor adapter protein 1 (LDLRAP1), a protein that influences LDL

uptake in the blood. Since this discovery, several other labs have found many more plant miRNAs regulating genes in mammals, reinforcing the existence of this pathway (Pirí et al., 2016; Yang et al., 2016; Chin et al., 2016; Yang et al., 2015; Pastrello et al., 2016; Zhou et al., 2014).

#### 1.4 PLANTS TO PRODUCE AND DELIVERY TUMOR SUPPRESSOR miRNAs

Because plants can be genetically engineered to produce miRNAs of any desired sequence, cross kingdom regulation by ingested plant miRNAs raised the possibility of using edible plants to produce therapeutic mammalian miRNAs that could be delivered via the diet to prevent or treat disease (Hirschi et al., 2015; Mlotshwa et al., 2015). Previous work from our lab tested this idea by feeding a daily dose of plant RNA spiked with a cocktail of mammalian tumor suppressor miRNAs (miR-34a, miR-143, miR-145) to *Apc<sup>Min/+</sup>* mice, a model for colon cancer. This treatment resulted in a highly statistically significant reduction in tumor burden in mice receiving the tumor suppressor miRNAs compared to controls (Mlotshwa et al. 2015). The miRNAs used in this study were not made in a plant, but synthetically made with a 2'-O-methylation at their 3' termini, a major characteristic of plant miRNAs, and meant to mimic miRNA produced in the plant. In this dissertation, this hypothesis is tested further, by establishing methods of bioengineering plants to produce mammalian tumor suppressor miRNAs, assaying their chemopreventive activity by feeding them to *Apc<sup>Min/+</sup>* mice, and characterizing the loading of miRNAs into plant exosome-like vesicles (EVs) for use as an efficient delivery vehicle.

## CHAPTER 2

### DESIGN OF MIRNA CONSTRUCTS AND GENERATION OF TRANSGENIC LINES

#### 2.1 INTRODUCTION

##### 2.1.1 USING PLANTS AS BIOFACTORIES TO PRODUCE THERAPEUTIC MIRNAS

The Vance lab pilot study showed that oral administration of plant RNA spiked with a cocktail of three mammalian tumor-suppressor miRNAs (miR-34a, miR-143, and miR-145), synthesized with the 3'-methylation characteristic of plant miRNAs, has significant chemopreventive activity in a mouse model of colon cancer (Mlotshwa et al., 2015). Based on this result, the first step in this dissertation project was to use the model plant *Arabidopsis thaliana* to produce the same three tumor suppressor miRNAs used in the earlier pilot study. *Arabidopsis* was chosen as it is well characterized, easily transformed, and edible (Clough and Bent, 1998). In addition, this technology has been patented by the Vance lab. The technology to produce any miRNA in bioengineered plants is well-established, simple, rapid and effective (Liang et al., 2012). The technique uses a natural plant miRNA precursor gene as the starting structure and replaces the natural miRNA sequence with the desired miRNA sequence, while also replacing the natural, partially complementary miRNA\* sequence to maintain the original secondary stem-loop structure of the precursor. Maintaining this secondary structure ensures

proper processing of the miRNA by Dicer like-1 (DCL1), a ribonuclease protein which functions in excising the mature miRNAs from the stem-loop (Werner et al., 2010; Song et al., 2010). The engineered miRNA genes are then cloned under the control of a strong constitutive promoter, the Cauliflower Mosaic Virus 35S promoter (CaMV 35S), and stably introduced into plants using standard transformation via *Agrobacterium tumefaciens*. Such engineered miRNAs are essentially indistinguishable from endogenous plant miRNAs regarding both biogenesis and function.

### 2.1.2 MAMMALIAN TUMOR SUPPRESSOR MIRNAS MIR-34A, MIR-143, MIR-145 AND THEIR ROLE IN CANCER

The three miRNAs chosen for these experiments are verified tumor suppressor miRNAs, which have been shown to be down regulated in several cancer types, including colon cancer (Gambari et al., 2016; Kano et al., 2010; Clapé et al., 2009). If these three miRNAs are added back either *in vivo* or *in vitro*, the disease can be prevented or progression can be inhibited, illustrating the importance of these small RNAs in chemoprevention (Pramanik et al., 2011). The miR-34a gene is a transcriptional target of the well-established tumor suppressor protein p53, and is consequently down-regulated in many tumor types and paired with several p53 downstream effects (Nalls et al., 2011). miR-143 and miR-145 are polycistronic, meaning they are expressed together on the same primary transcript, and often work synergistically to knock down several shared oncogenic

targets (Yan et al., 2014). Both of these miRNAs have been shown to positively regulate their own expression by targeting negative regulators (Wang et al., 2015).

## 2.2 RESULTS AND DISCUSSION

### 2.2.1 DESIGN APPROACHES FOR EXPRESSING MAMMALIAN THERAPEUTIC MIRNAS LARGER THAN 21NT IN *ARABIDOPSIS THALIANA*

A common approach for expressing miRNAs in plants uses the miR319a gene as backbone and replaces the natural miRNA sequence with the desired one. However, this approach is designed to work for miRNAs that are 21 nucleotides (nt) long, the length of the majority of plant miRNAs. This presented a problem when designing constructs to produce mammalian miRNAs in plants because mammalian miRNAs are often longer than 21 nt. Thus, it was necessary to develop strategies to ensure the proper processing of miR-34a and miR-145, which are 22 nt and 23 nt long, respectively. Two different approaches were used and both approaches had success in producing an extremely high level of the therapeutic miRNAs in *Arabidopsis thaliana*. miR-143 is a 21 nt miRNA; therefore, no special modifications of the standard technique were needed to engineer this miRNA.

The first design approach for making a miRNA longer than 21 nt involved making modifications to the miRNA\* region of the primary transcript. The stem-loop secondary structure of primary miRNA transcripts in plants plays an important role in recognition by DCL1 and proper processing to produce the mature miRNA. Several mismatches are often found between the miRNA and miRNA\* in the stem

loop structure, and maintenance of these mismatches is important in miRNA processing. If the mismatches are altered, either by changing their location in the stem loop or by altering them to complementary nucleotide pairs, it may disrupt proper miRNA production. The miR319a gene backbone has 3 mismatches between the miRNA and miRNA\*, found at nucleotides 1, 8, and 19 of the miRNA. A published protocol for plants has shown that modifications can be made to the miRNA\* of a 21 nt miRNA that will result in production of a 22 nt miRNA rather than the original 21 nt one (Song et al., 2010). The modification consists of creating a deletion in the miRNA\* sequence at the position of an existing mismatch in the miRNA/miRNA\* duplex. Although this modification makes a bulge in the secondary structure, it does not adversely affect the processing function of DCL1. Applying this approach, designs for generating the longer miR-34a and miR-145 miRNAs were made.

Due to the challenges in designing a miRNA over 21 nt long using the miR319a gene backbone, a second strategy for generating mammalian miRNAs in plants was also tried. This approach was to simply make a 21 nt version of the mammalian miRNA by leaving off nucleotides from the 3' end of the miRNA. This is a valid approach because it has been reported that nucleotides lost from the 3' end of the miRNA have little to no effect on targeting specificity of the miRNA (Grimson et al., 2007). This is because specificity is primarily determined by the miRNA seed sequence, a highly conserved region in mammalian miRNAs located from nucleotides 2 – 7 of the 5' end (Lewis et al., 2005). This approach was the

one ultimately used to produce miR-34a, with one nucleotide being removed from the 3' end, thereby shortening the plant-produced version to 21 nt.

## 2.2.2 CLONING MIRNA CONSTRUCTS AND GENERATION OF TRANSGENIC LINES

The engineered miR-143 21 nt and miR-34a 21 nt were designed using the standard protocol, in which the plant miR319a gene is used as a backbone, with the appropriate miR/miR\* sequences replacing the original miR319a/miR319a\* sequences (Figure 2.1). The 23-nt miR-145 and the 22-nt version of miR-34a were more complicated because of their length, and several different constructs were evaluated in order to improve the chances of obtaining the correct sized miRNAs. These constructs had deletions made along their miRNA\* region, but the only construct that produced the correct size miRNA was miR-145 23nt that had 2 deletions at the 17 nt position of the miRNA (Figure 2.2; data not shown for some constructs). Because the miR391a gene sequence is relatively short (406bp), the appropriate complete DNA constructs were synthesized and cloned directly into an entry vector (pENTR). To check for sequence accuracy, each miRNA construct was sequenced. Constructs with the correct sequences were used in a recombination reaction to transfer the insert into an expression vector (pSITE-OA), and subsequently sequenced again before transformation into *Agrobacterium tumefaciens*, for transfer to plants. *Arabidopsis thaliana* was transformed by *Agrobacterium*-mediated transformation using the floral dip method (Martinez-Trujillo et al., 2004). Because the inserted DNA carries a specific antibiotic

resistance, the primary plant transformants (T1 generation) could then be selected by plating seeds from the floral dip procedure onto media with the selective antibiotic. Resistant seedlings (primary transformants) were transplanted into soil for seed set, and the T2 generation seeds were plated again on selective media. Transformants segregating 3:1 for antibiotic resistance were identified as putative single insertion lines for further characterization. Seeds from these plants (T3 generation) were again selected for antibiotic resistance to identify homozygous lines, which were then used to produce bulk seed (T4 generation) for the feeding and exosome isolation experiments described in the next two chapters. RNA was isolated from each of these homozygous lines, and expression levels of the engineered miRNA was determined by RNA gel blot analysis using radioactive probes specific for the small RNA. Homozygous plant lines expressing the highest levels of each engineered miRNA of the correct size were used for the reported experiments, and are also available for future studies.

### 2.2.3 CHARACTERIZATION OF PLANT-MADE miR-34A, miR-143 AND miR-145 BY NORTHERN ANALYSIS AND NEXT GENERATION SEQUENCING

The population of miRNA size variants (isomiRs) for each of the tumor suppressor miRNAs produced by transgenic plant lines, as well as that for the endogenous plant miRNA miR319, was analyzed by next generation sequencing. The relative abundance of endogenous plant miR319a small RNAs (64%) were the reported 21nt sequence, with 27% a single nucleotide shorter (Figure 2.4A). The two plant lines that were engineered to make a 21 nt miRNA (miR-143 and

the 21 nt version of miR-34a), like the endogenous miR319, both made high levels of the desired 21 nt small RNA (45% and 49%, respectively), with the majority of the remainder being a single nucleotide shorter (50% and 32%, respectively); Figures 2.4B and C). Northern blot data showed that plants transformed with the 23 nt miR-145 constructs produced a ~23 nt miRNA at a high level in a stably transformed homozygous *Arabidopsis thaliana* line. When examined by next generation sequencing, the major variant was the desired size of 23 nt (57%), with a population of 25 nt miRNA representing 27% of the size distribution (Figure 2.4D). None of the miR-34a lines designed to be 22 nt, however, produced a 22 nt miRNA at high level (Northern analysis; data not shown).

This work illustrates two approaches to produce exogenous miRNAs in plants when the natural size of the miRNA is greater than 21 nt. Based on next generation sequencing, it appears that both approaches result in a population of small RNA isomiRs of slightly different sizes. Though all constructs produced a population of size isomiRs, this is quite common in nature, as illustrated here by the endogenous plant miR319a. The approach of designing a larger miRNA by deleting nucleotides in the miRNA\* appears to be successful in some cases (miR-145), but not in others (miR-34a). The fall back approach, then, in the event that the first approach is not successful, is to simply design a 21 nt version of the desired miRNA by leaving off nucleotides from the 3' end.

<b>A</b>		miR319a 21nt		
miR*	3'		5'	
miR	5'		3'	
<hr/>				
<b>B</b>		U	U	A
miR319a	miR*	3' acu	UUCUUC GCACGACGAA	Uaaga 5'
21nt	miR	5' uga	AAGAAG CGUGCUGCUU	AUucu 3'
		U	U	C
<hr/>				
<b>C</b>		U	A	A
miR143	miR*	3' acu	CUCUAC UCGUGACAUC	AGaga 5'
21nt	miR	5' uga	GAGAUG AGCACUGUAG	UCucu 3'
		U	A	C
<hr/>				
<b>D</b>		C	G	U
miR34a	miR*	3' acu	CCGUCA AGAAUCGACC	ACaga 5'
21nt	miR	5' uga	GGCAGU UCUUAGCUGG	UGucu 3'
		U	G	U
<hr/>				
Nucleotides		1	8	19

**Figure 2.1: miRNA/miRNA\* region of miRNA constructs.** Shown are the miRNA/miRNA\* sequences (capital letters) for each of the miRNA constructs in the miR319a backbone **(A)** endogenous miR319a miR/miR\* with mismatches at the 1 nt, 8 nt, 19 nt positions used as a blueprint for mismatches in 21 nt constructs **(B)** miR319a **(C)** miR-143 21 nt construct **(D)** miR-34a 21 nt construct



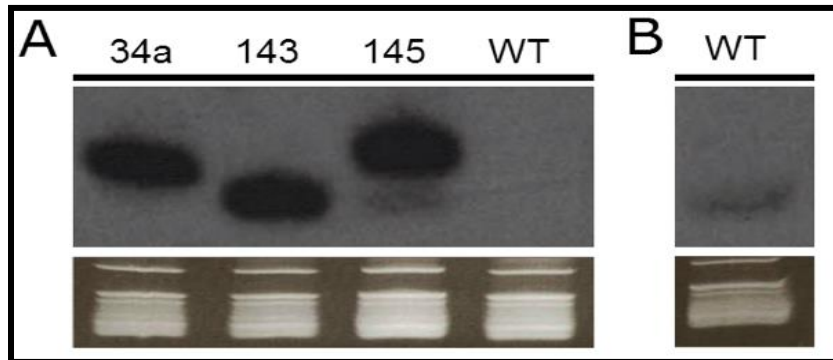


**Figure 2.3: Production of three mouse miRNAs in bioengineered plants.** Gel blot analysis of RNA samples isolated from wild type (WT) *Arabidopsis* and homozygous lines expressing miR-34a, miR-143 or miR-145. **(A)** The blot was probed for all three tumor suppressor miRNAs. **(B)** A duplicate WT sample was probed for the highly expressed endogenous plant miRNA, miR168a. The ethidium bromide (EtBr) stained gel is shown as loading control below the autoradiograms.

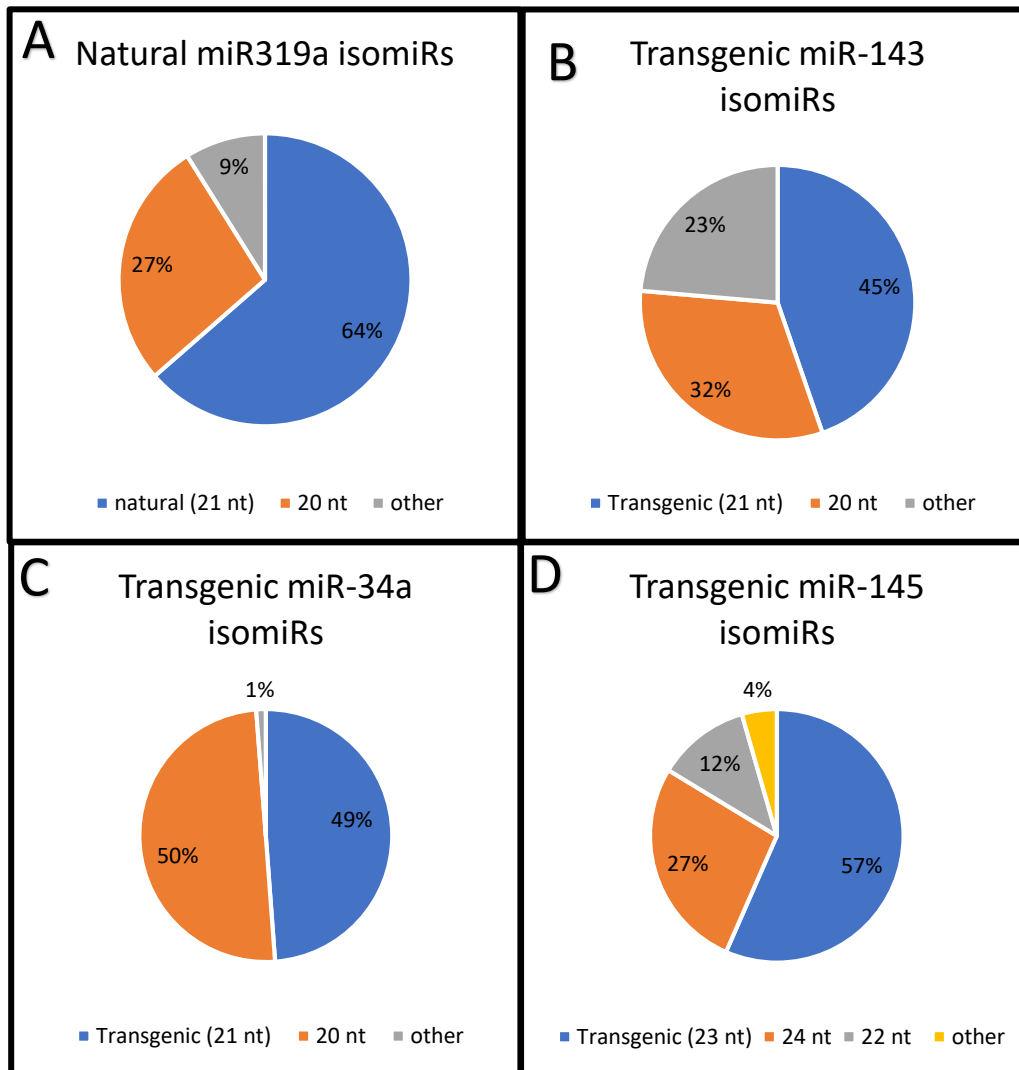


**Figure 2.4: miRNA isomiR distributions in bioengineered plants.** Shown are the miRNA isomiR distribution in each independent homozygous *Arabidopsis* line analyzed by next generation sequencing **(A)** endogenous miR319a isomiR distribution **(B)** miR-34a 21 nt isomiR distribution **(C)** miR-143 isomiR distribution **(D)** miR-145 23 nt isomiR distribution

## CHAPTER 3

### FEEDING EXPERIMENT: DIETARY DELIVERY OF MAMMALIAN TUMOR SUPPRESSOR MIRNAS

#### 3.1 INTRODUCTION

##### 3.1.1 RESTORATION OF TUMOR SUPPRESSOR MIRNAS VIA INGESTION OF BIOENGINEERED ARABIDOPSIS

In the published Vance lab pilot experiment, *Apc<sup>Min/+</sup>* mice were gavaged with total plant RNA spiked with three validated tumor suppressor miRNAs (miR-34a, miR-143, and miR-145) synthesized to have the methylation characteristic of miRNAs produced in plants (Mlotshwa et al., 2015). The experimental approach was to use a preventive regimen, with treatment starting before the mice developed polyps. After five weeks of daily gavage, the tumor burden in the miRNA-treated mice was significantly reduced compared to mice that didn't receive the miRNAs. Based on these results, a feeding experiment was proposed which would replicate the design of the pilot experiment, but use miRNAs actually produced in transgenic plants rather than synthetic ones, and also deliver the miRNAs by incorporating the transgenic plant material into the *Apc<sup>Min/+</sup>* mouse diet.

### 3.1.2 RATIONALE FOR CHOICE OF DISEASE AND MOUSE MODEL

Colorectal cancer (CRC) is the third leading cause of cancer death in both men and women. Approximately 140,000 people in the US will be diagnosed with the disease in 2018 and over 50,000 will die from it (Siegel et al., 2018). Even though new screening techniques and advances in surgical treatment have reduced the mortality rate of CRC, there is almost a 50% chance of reoccurrence of the disease post-surgery, and greater than one third of the people who develop the disease will die from it. Mortality rates have declined over the last decade due to several factors, like decreased smoking, maintaining a healthy weight, reduced red meat consumption, regular colorectal screenings and improved treatments (Fedewa et al., 2015). Though preventative screenings can greatly reduce the risk of ever developing CRC, many people avoid the procedure due to its invasiveness and cost (Zauber, 2015). Another disturbing trend is the rise of CRC cases seen in adults <50 years old, where both CRC incidences and mortality rates have been reported to increase (Bhandari et al., 2017). These statistics illustrate the need for new preventive strategies, and delivery of tumor suppressor miRNAs via the diet, if successful, could have a big impact. The *Apc<sup>Min/+</sup>* mouse is an *in vivo* model for CRC (Corpet and Pierre, 2003), which has a heterozygous truncation of the *Apc* gene. Because similar mutations in the *Apc* gene occur in about 80% of cases of CRC in humans, the *Apc<sup>Min/+</sup>* mouse is an excellent *in vivo* model for human CRC (Haggar and Boushey, 2009). The mice develop numerous tumors in the intestine and are commonly used to test chemopreventive therapies for CRC because the

effect of therapies can easily be assayed by determining the effect on number of tumors (Perkins et al., 2002).

### 3.1.3 THE RATIONALE FOR CHOICE TUMOR SUPPRESSOR MIR-34A, MIR-143, AND MIR-145

The experimental approach for the earlier pilot study was to use three different validated tumor suppressor miRNAs to optimize the chances of a successful intervention. Based on the success of the pilot, the same combination of tumor suppressors was chosen for the feeding experiment. Two of the three miRNAs, miR-143 and miR-145, are co-expressed on the same primary transcript, and often work synergistically to knock down several shared oncogenic targets (Akao et al., 2010). They are downregulated early in CRC development (Weng et al., 2015), and restoration of their levels inhibits growth of CRC cells in culture. In contrast, overexpression of the two miRNAs reduces the development of tumors in *Apc<sup>Min/+</sup>* mice (Takaoka et al., 2012). The fact that these two miRNAs are naturally co-expressed and act synergistically justifies administering the two together for our experimental approach.

The third miRNA, miR-34a, has broad activity as a tumor suppressor in many tumor types (Nalls et al., 2011). It has been found to regulate targets in important cell cycle pathways, such as CDK6 in the p53 pathway and Notch 1 in the Wnt signaling pathway (Saito et al., 2015). In contrast to miR-143 and miR-145, it is down regulated a later stage of CRC progression, and may play a role in cells acquiring the ability to spread and invade other organs (Jin et al., 2015).

Restoration of miR-34 levels has been shown to induce cell apoptosis, cell cycle arrest, and p53 transcription *in vivo*, making it a strong candidate for chemopreventive approaches (Saito et al., 2015).

## 3.2 RESULTS AND DISCUSSION

### 3.2.1 DEVELOPING METHODS FOR DIETARY DELIVERY OF MAMMALIAN TUMOR SUPPRESSOR MIRNAS PRODUCED IN BIOENGINEERED *ARABIDOPSIS THALIANA*

Two major challenges had to be overcome before it was possible to do the feeding experiment. First, a method was needed to allow miRNAs from plant material to remain functional for long periods of time without degrading, as RNA is relatively unstable and prone to breakdown (Garneau et al., 2007). Second, a way was needed to incorporate the miRNAs into the mouse diet without using too great a mass of plant tissue. Initially, using juice instead of plant tissue was tested. To test juicing, bioengineered *Arabidopsis* was processed using a commercially available juicer that separated the solid plant material from the liquid. However, a large portion of the bioengineered miRNA was lost with the solid material, and the remaining miRNA was unstable in juice, degrading within 24 hours at 5°C (Figure 3.2).

An alternative approach to reduce the mass of plant material for incorporation into mouse chow, while also stabilizing the miRNA, was lyophilization. The method chosen was lyophilization. To test this approach, fresh *Arabidopsis* leaves expressing bioengineered miR-34a 21 nt were frozen in liquid

nitrogen, ground briefly with a mortar and pestle, and lyophilized until sublimation was complete. This method not only stabilized the miRNAs for up to 4 weeks while stored at room temperature, it reduced the total weight of the plant material by 10-fold (Figure 3.3). Thus, one gram of lyophilized plant material contained the same amount of miRNA as ten grams of fresh tissue.

Feeding the lyophilized plant tissue to mice meant it had to be incorporated into mouse chow, an intense procedure that involves heating. The stability of miRNAs during incorporation into mouse chow was tested by mixing lyophilized plant tissue with commercial standard AIN-76A mouse synthetic diet (a mixture that is similar to purified components that would be added to the plant material to make a balanced diet), adding water, compacting the mixture, and heating it for 8 hours at 46°C. Lyophilization was able to stabilize the miRNAs during the simulated chow incorporation process (Figure 3.4). Because miRNA levels were unaffected by lyophilization, total plant mass was reduced 10-fold, and degradation was not seen during the simulated diet incorporation process, this was the method selected for dietary delivery of plant-produced miRNAs.

### 3.2.2 DESIGN OF HEALTHY MOUSE TEST DIETS

Lyophilized plant material was analyzed by a commercial company to determine the levels of macronutrients and micronutrients in preparation for having custom mouse diets made by a commercial supplier (Table 3.1). Based on the results from the nutritional analysis of lyophilized *Arabidopsis*, two healthy mouse diets were designed, one diet incorporating 10% *Arabidopsis*, and a diet that was

matched calorically and nutritionally, but did not contain plant tissue (purified diet). This was achieved by mixing together a set of purified ingredients (Table 3.2), taking the input of the *Arabidopsis* into consideration, and ensuring the nutritional and caloric components of the two diets were matched (Table 3.3). A bacon flavor additive was used to increase palatability. The *Arabidopsis* diet contained 3.33 g of each of the lyophilized homozygous lines bioengineered to express one of the mammalian tumor suppressor miRNAs (miR-34a 21 nt, miR-143 and miR-145 23 nt), totaling 10 g per 100 g of chow. miRNAs are stable for two weeks room temperature after incorporation into mouse chow, and the purified diet contained no miRNAs (Figure 3.6).

### 3.2.3 DIET CONTAINING BIOENGINEERED ARABIDOPSIS HAD SIGNIFICANT CHEMOPREVENTATIVE ACTIVITY IN *APC<sup>Min/+</sup>* MICE

The feeding experiment used two groups of six male *Apc<sup>Min/+</sup>* mice fed either the transgenic plant diet bioengineered to produce three tumor suppressor miRNAs or the control nutritionally and calorically matched purified diet without miRNAs. Mice from the two groups were weaned onto their respective diets in a preventative regimen (starting at three weeks of age), and weights of the mice were taken weekly, which showed that the mice in the two groups gained weight at the same rate (Figure 3.7A). The weight of the food consumed per group was recorded as well, showing mice on the two different diets consumed approximately the same amount of food (Figure 3.7B). Mice were sacrificed after six weeks on the diet (at nine weeks of age), and the number of tumors in the small and large

intestine counted after methylene blue staining. Mice that consumed the diet containing *Arabidopsis* bioengineered to express mammalian tumor suppressor miRNAs had significantly fewer tumors ( $p=.0454$ ) than mice fed the matched purified diet (Figure 3.7). Mice fed the transgenic plant diet had an average of 21 tumors (SD 4.179), while the mice on the purified diet had an average of 32.83 tumors (SD 4.74). Thus, ingestion of plant tissues engineered to produce tumor suppressor miRNAs had a statistically significant chemopreventive impact.

#### 3.2.4 *APC*<sup>MIN/+</sup> MICE FED THE MIR DIET HAD ELEVATED LEVELS OF MIR-34A, MIR-143, AND MIR-145 COMPARED TO THE CONTROL GROUP

Next generation sequencing was used to determine if the reduced tumor burden observed in the mouse group receiving the transgenic plant diet, also showed an increase in the level of the dietary miRNAs in intestinal tissues. RNA was isolated from a 2cm proximal section scraping of the small intestine to measure levels of the administered miRNAs using next generation sequencing. The two groups had their RNA samples pooled and prepared using equal amounts of RNA from the individual members of the group: the transgenic plant diet group (containing miRNAs) and the control purified diet group (without miRNAs). Next generation sequencing was performed on the two pooled group samples, and the number of reads of known miRNAs, as normalized to reads per million, was determined. The group receiving the transgenic plant diet had higher levels of all three administered miRNAs than those from the group receiving the control purified diet; however, the levels of miRNAs that were not administered via the transgenic

plant diet did not differ between the two groups (Figure 3.8A). This result raised the possibility that the increased level of the engineered miRNAs detected in the plant-fed mice might reflect dietary uptake of the miRNAs. However, the possibility that uptake of plant-produced miRNA directly accounts for the observed increase in sequence reads is unlikely because of the strong bias against detection of the methylated plant-produced miRNAs in a background of mammalian miRNAs, which do not have inhibiting 2'-O-methylation at the 3' end (Raabe et al., 2014). In addition, the increases in miR-143 and miR-145 were substantial, arguing against attributing them to dietary uptake. Another possibility is that the dietary miRNAs were taken up by the intestinal cells, and, although they could not be directly detected due the methylation bias, were active in the mouse tissue. One consequence of their activity is that a positive feedback loop for miR-143/miR-145 would be triggered and result in up-regulation of the expression of the endogenous gene encoding the two miRNAs (Pagliuca et al., 2013; Takaoka et al., 2012). This scenario would explain the observed increase in the administered miRNAs as well as the reduced levels of their known direct target mRNAs reported below.

### 3.2.5 *APC<sup>MIN/+</sup>* MICE FED THE MIR DIET HAD DECREASED LEVELS OF TARGETS OF MIR-34A, MIR-143, AND MIR-145 COMPARED TO THE CONTROL GROUP

An increase in the levels of the administered tumor suppressor miRNAs would be predicted to result in a decrease in at least some of the direct targets of those miRNAs. To determine if known targets were reduced, the same pooled

RNA group samples used to measure levels of miRNAs, were analyzed by RNA seq to determine mRNA levels. Several well-established targets of miR-34A, miR-143, and miR-145 were found at reduced levels in the transgenic plant diet group compared to those in the control synthetic diet group (Figure 3.9), including eight known miR-143 targets (Figure 3.9A), five known miR-145 targets (Figure 3.9B), and six known miR-34a targets (Figure 3.9C) (Davis-Dusenbery et al., 2011; Kent et al., 2014; Zhang et al., 2009; Qian et al., 2013; Xu et al., 2017; Chen et al., 2009; Cui et al., 2014; Manuscript and Dysfunction, 2015; Chou et al., 2016). These data are consistent with the increased levels of the administered miRNAs observed in the plant diet group compared to the control purified diet group, suggesting that the detected miRNAs represent an active population. It should be noted that these 3 miRNAs have many targets, miR-34a has over 700 confirmed targets alone, the targets examined were randomly selected based on the literature (Slabáková et al., 2017).

Overall, these results show that mice fed a diet containing bioengineered *Arabidopsis* expressing mammalian tumor suppressor miRNAs had a statistically significant reduction in tumor burden compared to those fed a nutritionally and calorically matched synthetic diet. In addition, when pooled RNA samples from the two groups were analyzed by next generation sequencing, the levels of the three administered miRNAs was increased in the plant-fed group compared to the control group, suggesting uptake of dietary miRNAs. Furthermore, the increased levels in the three administered miRNAs was accompanied by decreases in numerous known direct targets of the miRNAs. These results look promising for

the use of plants as biofactories to produce and deliver dietary miRNAs. However, limitations in the experimental approach prevent drawing firm conclusions at this time. First, the RNA sequencing data used pooled samples, so the statistical significance of the results cannot be determined. Second, the chemopreventive impact of the diet cannot definitively be attributed to the bioengineered miRNAs produced by the plant. To unravel the role of the plant itself from the bioengineered miRNAs would require including an additional control group receiving the same level of non-transgenic plant tissue. Whereas the decreased tumor burden in the plant-fed group cannot be directly attributed to the tumor suppressor miRNAs produced by the plant, the increased levels of the bioengineered miRNAs in mouse intestinal samples of the plant-fed group and the accompanying decrease in levels of their direct targets, suggest that the observed chemopreventive effect may be mediated by the dietary miRNAs. Future studies should use larger sample size, analyze individuals rather than pooled samples, and include a control group fed non-transgenic plant material to tease out the roles of the plant versus the bioengineered miRNAs.

This experiment also raised the point that there may be a limit to the amount of lyophilized plant tissue that can be incorporated into a diet before the food becomes unpalatable. Therefore, methods aimed at increasing the concentration of miRNAs in the sample, while simultaneously decreasing overall plant mass, are needed. One such method may lie in a proposed delivery mechanism for plant-made miRNAs: plant exosome-like vesicles (EVs). Plant EVs, and the mechanisms that controls loading of miRNAs into them, are discussed in the next chapter.

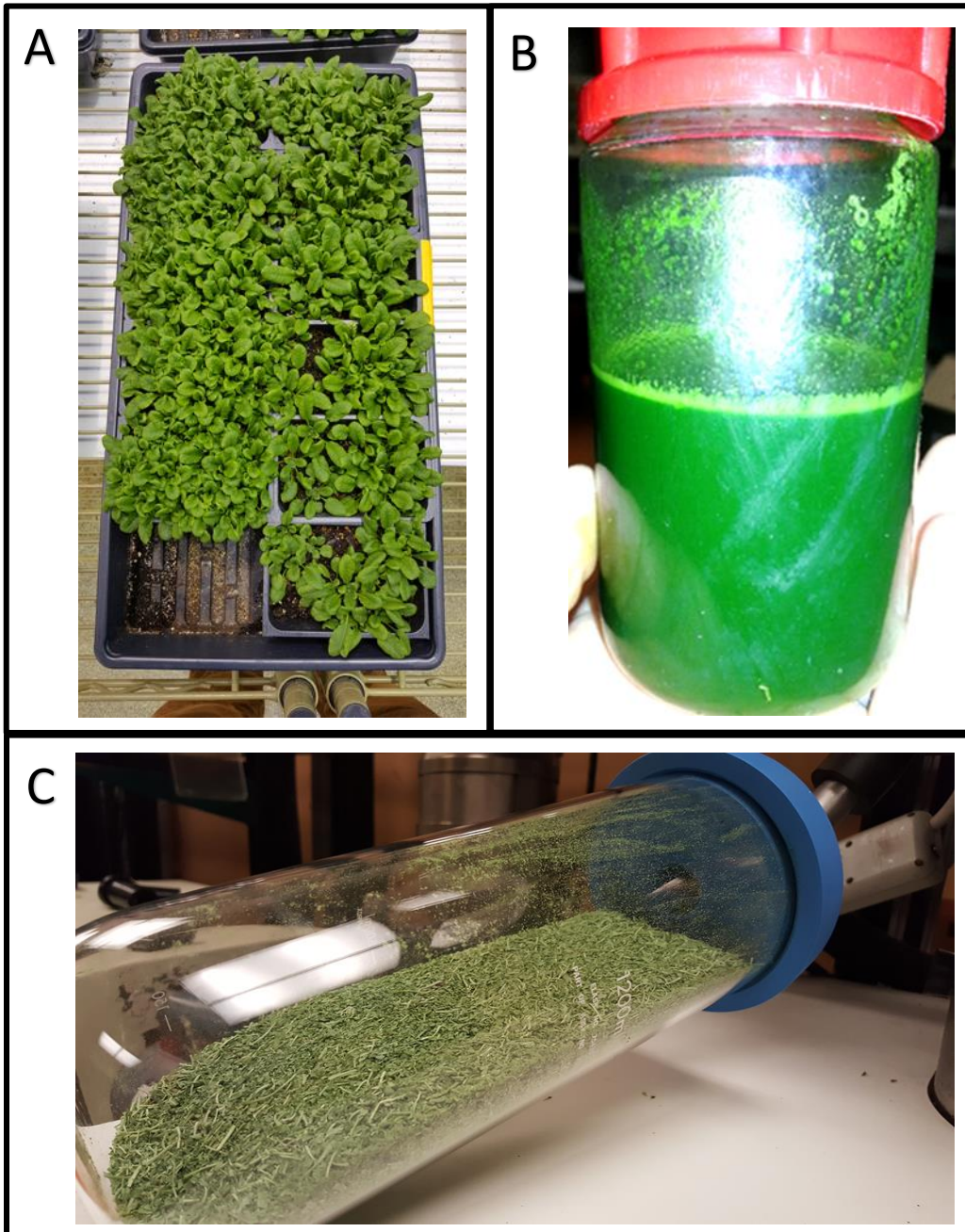


**Figure 3.1: Images of leaves, juice, and lyophilized *Arabidopsis*.** Three different tissue preparations for *Arabidopsis thaliana*. (A) Fresh *Arabidopsis* leaves (B) *Arabidopsis* just after juicing and before a low speed centrifuge spin (C) *Arabidopsis* shortly before lyophilization is complete.

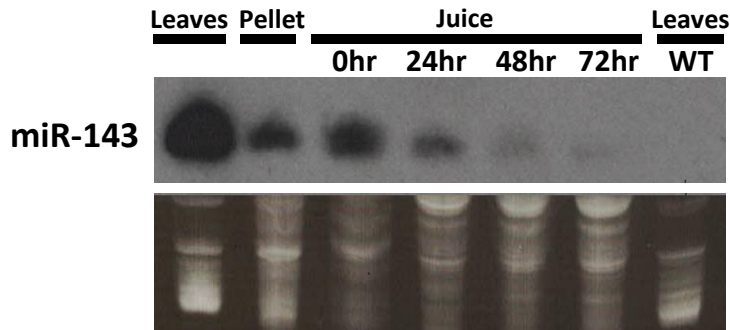


**Figure 3.2: miR-143 stability in juice.** Gel blot analysis of RNA samples isolated from *Arabidopsis* homozygous line expressing miR-143 and WT. Time course shows stability of miR-143 after juicing and storage at 5°C compared to fresh WT *Arabidopsis* and *Arabidopsis* expressing miR-143. The ethidium bromide (EtBr) stained gel is shown as loading control below the autoradiograms.

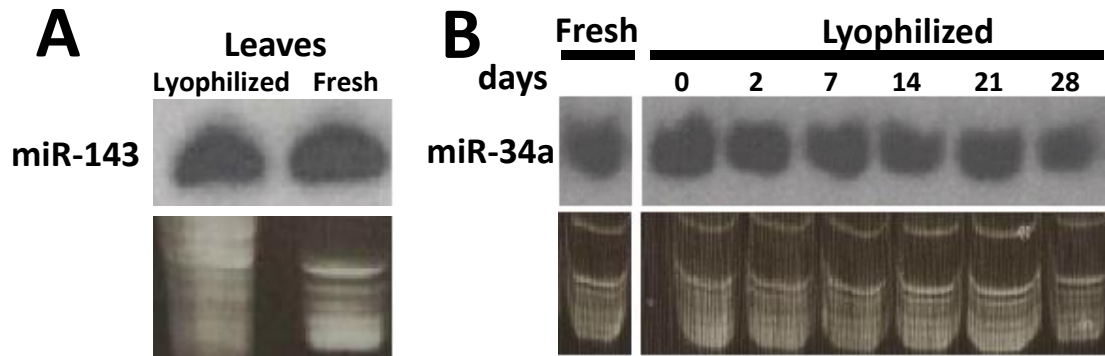


**Figure 3.3: miR-143 and miR-34a stability in lyophilized plant tissue.** Gel blot analysis of RNA samples isolated from fresh and lyophilized *Arabidopsis* bioengineered to express miR-143 and miR-34a **(A)** miR-143 expression level in fresh *Arabidopsis* and immediately after lyophilization. **(B)** Time course shows stability of miR34a after lyophilization and storage at room temperature compared to fresh *Arabidopsis*. The ethidium bromide (EtBr) stained gel is shown as loading control below the autoradiograms.

miR159a

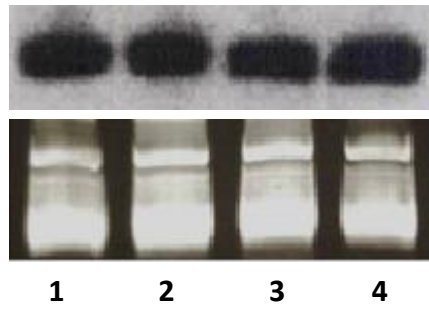


**Figure 3.4: Stability of endogenous plant miR-159a during mouse chow incorporation.** Gel blot analysis of RNA samples isolated from lyophilized *Arabidopsis* stored at  $-80^{\circ}\text{C}$ . Lyophilized plant tissue was subjected to mixture with a raw AIN-76A diet, adding water, and pressure by crushing in a mortar and pestle, and tested at  $46^{\circ}\text{C}$  and room temperature condition. **(Lane1)** RNA isolated from lyophilized leaves **(Lane2)** RNA isolated from lyophilized leaves mixed with an AIN 76a diet mixture, water, and left at room temperature for 8 hours **(Lane3)** RNA isolated from lyophilized leaves mixed with an AIN 76a diet mixture, water, and heated at  $46^{\circ}\text{C}$  for 8 hours **(Lane4)** RNA isolated from lyophilized leaves mixed with an AIN 76a diet mixture. The ethidium bromide (EtBr) stained gel is shown as loading control below the autoradiograms.

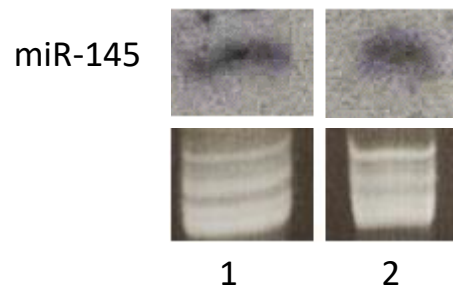


**Figure 3.5: miRNAs are stable in mouse chow incorporated in 10% *Arabidopsis* diet.** RNA was isolated from mouse chow containing 10% *Arabidopsis* after being sent out overnight on dry ice to be incorporated into chow, then sent back overnight on dry ice and stored at -80°C. **(Lane 1)** miR diet taken out of -80°C storage and a RNA isolation was performed. **(Lane 2)** miR diet was stored at room temperature for 2 weeks and another RNA isolation was performed. The ethidium bromide (EtBr) stained gel is shown as loading control below the autoradiograms

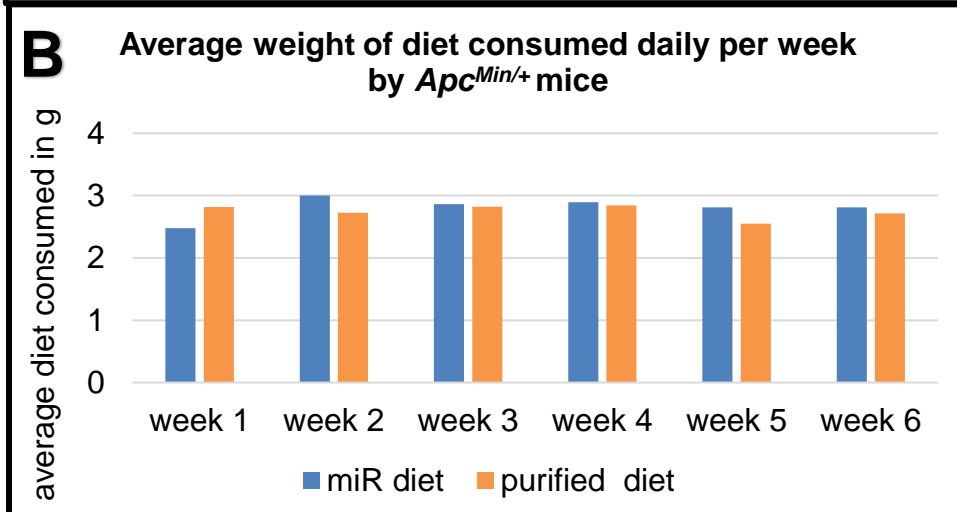
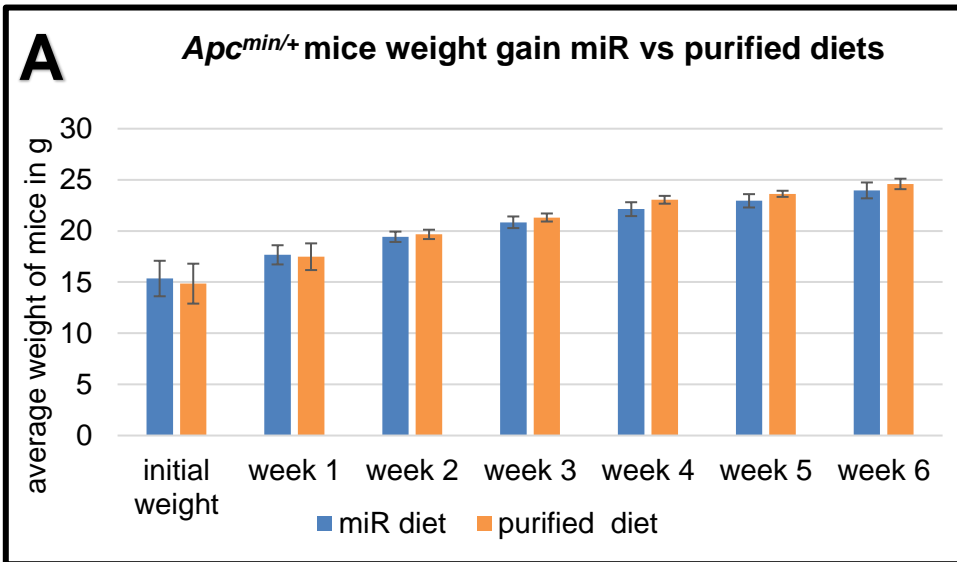


**Figure 3.6: Average weight of *Apc<sup>Min/+</sup>* mice and average weight of diets consumed.** The weight of mice and the chow they consumed was recorded weekly. **(A)** Weights of 3-week-old mice were taken initially before being weaned onto their perspective diets. Weights were recorded weekly, with mice being sacrificed immediately after the week 6 weighing. **(B)** The amount of diet each test group consumed was recorded weekly. Mice were fed in a collective manner, so total weight of food eaten was divided by the total number of mice per cage then divided by 7 days a week.

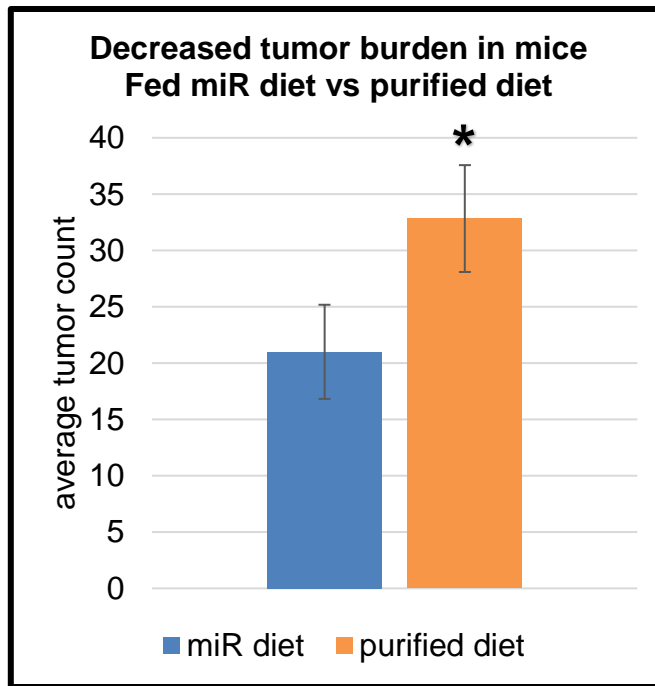


**Figure 3.7: Average *Apc<sup>Min/+</sup>* mice tumor burden in mice consuming 10% miR or purified diets.** The small and large intestine was removed from mice, flushed with PBS, fixed with formaldehyde, and stained methylene blue. A one tailed t tested showed significantly less tumors in the mice fed the miR diet compared to those on the purified diet (>0.04536).

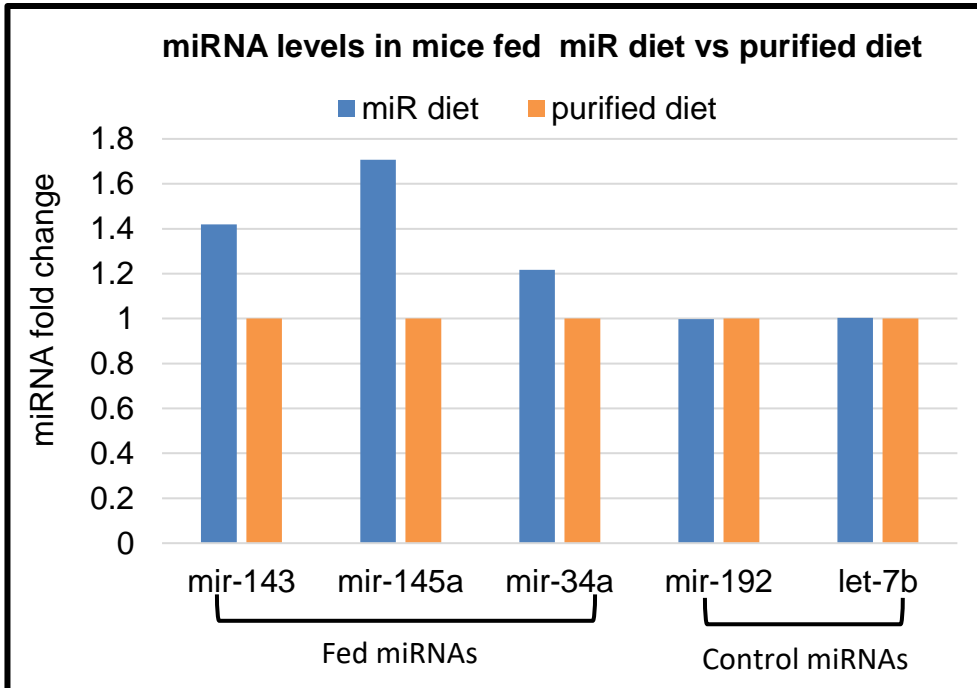


**Figure 3.8: Fold change of miRNAs in mice fed miR and purified diets.** Next generation sequencing of miRNAs and miRNA targets was performed on pooled RNA samples from mice fed miR and purified diets. Fold change was calculated from reads normalized to read per million. Fold change of miR-143, miR-145, and miR-34a in mice fed the miR and purified diets, miR-192 and let-7b that are highly expressed control miRNAs

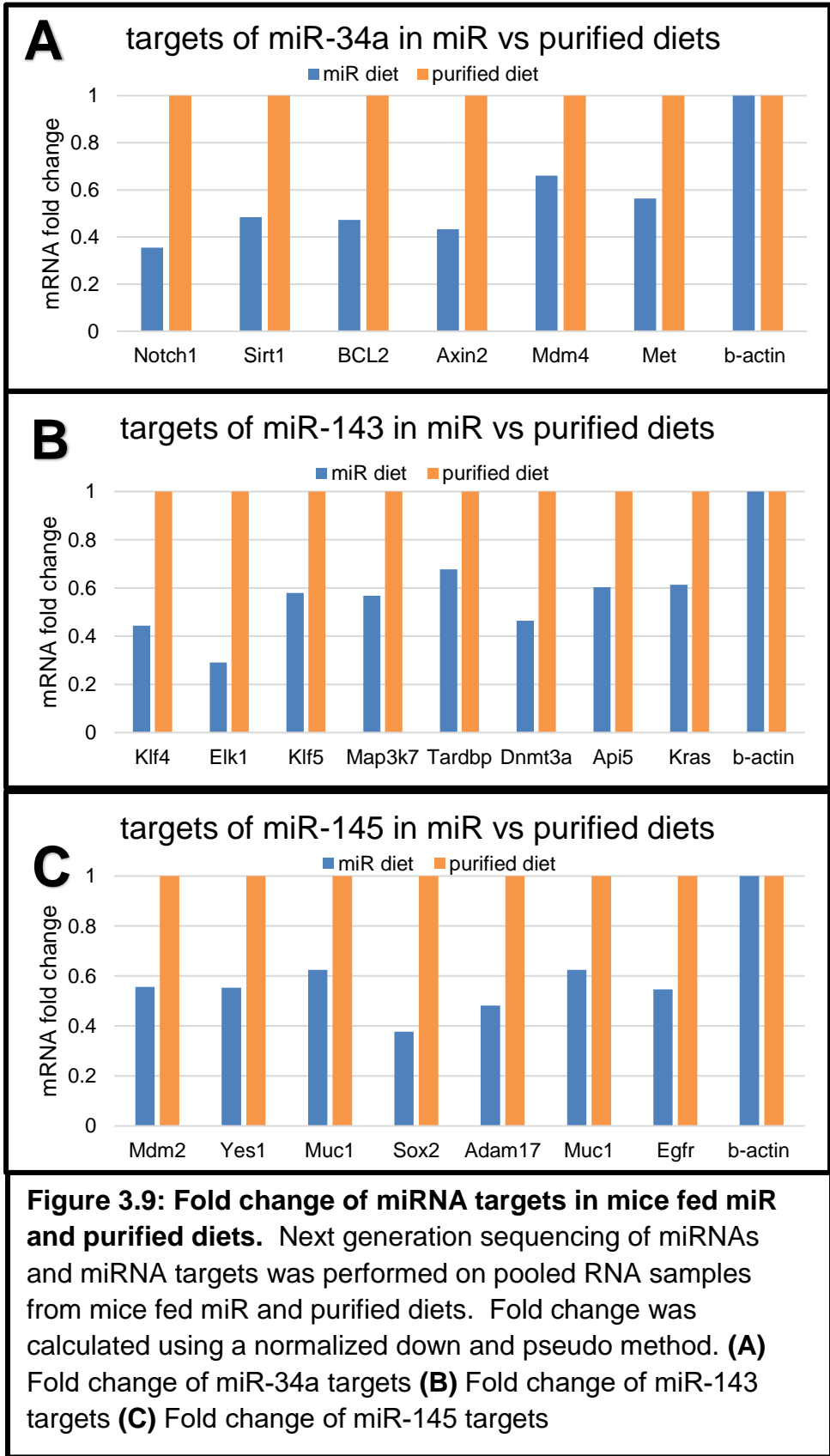


**Table 3.1: nutritional and caloric values of lyophilized *Arabidopsis***

<b>Fatty Acids Calculated as Triglycerides</b>		<b>Vitamin C (by HPLC)</b>		<b>Cholesterol</b>	
Saturated Fatty Acids	0.0846 g/10g	Vitamin C	48.9 mg/10g	Cholesterol	0.093 mg/g
Unsaturated Fatty Acids	0.0854 g/10g	<b>Elements by ICP ES</b>		<b>Carbohydrates</b>	
Monounsaturated Fatty Acids	0.0154 g/10g	Aluminum	1.76 mg/10g	Total Carbohydrates	2.85 g/10g
Polyunsaturated Fatty Acids	0.0700 g/10g	Barium	0.390 mg/10g	<b>Total Dietary Fiber</b>	
Trans Fatty Acids	0.0646 g/10g	Boron	0.497 mg/10g	Total Dietary Fiber	2.10 g/10g
Omega 3 Fatty Acids	0.0484 g/10g	Calcium	328 mg/10g	<b>Sugar Profile</b>	
Omega 6 Fatty Acids	0.0247 g/10g	Chromium	<39.7 mcg/10g	Fructose	0.02 g/10g
Omega 9 Fatty Acids	0.0071 g/10g	Copper	0.0916 mg/10g	Glucose	0.04 g/10g
Total Fatty Acids	0.245 g/10g	Iron	2.43 mg/10g	Sucrose	<0.01 g/10g
4:0 Butyric	<0.0007 g/10g	Magnesium	99.2 mg/10g	Lactose	<0.01 g/10g
6:0 Caproic	<0.0007 g/10g	Manganese	1.34 mg/10g	Maltose	<0.01 g/10g
8:0 Caprylic	<0.0007 g/10g	Molybdenum	<39.7 mcg/10g	Galactose	<0.01 g/10g
10:0 Capric	<0.0007 g/10g	Phosphorus	86.0 mg/10g	Total Sugar	0.06 g/10g
12:0 Lauric	<0.0007 g/10g	Potassium	463 mg/10g	<b>Protein (N x 6.25) Dumas Method</b>	
14:0 Myristic	<0.0007 g/10g	Sodium	8.14 mg/10g	Protein	4.54 g/10g
14:1 Myristoleic	<0.0007 g/10g	Strontium	1.07 mg/10g	Nitrogen	0.727 g/10g
15:0 Pentadecanoic	<0.0007 g/10g	Zinc	0.771 mg/10g	<b>Choline</b>	
15:1 Pentadecenoic	<0.0007 g/10g	<b>Amino Acids</b>		Choline	4.7 mg/10g
16:0 Palmitic	0.0782 g/10g	Aspartic Acid	273 mg/10g	<b>Calories</b>	
16:1 Palmitoleic	<0.0007 g/10g	Threonine	121 mg/10g	Calories	31.8 Cal/10g
17:0 Heptadecanoic	<0.0007 g/10g	Serine	123 mg/10g	<b>Calories from Fat</b>	
17:1 Heptadecenoic	<0.0007 g/10g	Glutamic Acid	356 mg/10g	Calories	2.21 Cal/10g
18:0 Stearic	0.0053 g/10g	Proline	126 mg/10g	<b>Fat by Acid Hydrolysis</b>	
9c 18:1 Oleic	0.0071 g/10g	Glycine	145 mg/10g	Fat	0.58 g/10g
18:2 Linoleic	0.0247 g/10g	Alanine	152 mg/10g	<b>Vitamin D by LCMS</b>	
20:0 Arachidic	0.0009 g/10g	Valine	157 mg/10g	Total Vitamin D3	<0.400 IU/10g
18:3 Gamma Linolenic	<0.0007 g/10g	Isoleucine	122 mg/10g	<b>Vitamin E (Natural)</b>	
20:1 Eicosenoic	<0.0007 g/10g	Leucine	230 mg/10g	Vitamin E	1.27 IU/10g
18:3 Linolenic	0.0484 g/10g	Tyrosine	101 mg/10g	<b>Vitamin K1</b>	
18:4 Octadecatetraenoic	<0.0007 g/10g	Phenylalanine	155 mg/10g	Vitamin K1	480 mcg/10g
20:2 Eicosadienoic	<0.0007 g/10g	Lysine	166 mg/10g	<b>Thiamin by Fluorometric Method</b>	
22:0 Behenic	0.0014 g/10g	Histidine	54.6 mg/10g	Thiamin	0.008 mg/10g
22:1 Erucic	<0.0007 g/10g	Arginine	142 mg/10g	<b>Riboflavin by Microbiological Method</b>	
20:3 Eicosatrienoic	<0.0007 g/10g	Cystine	19.2 mg/10g	Riboflavin	0.302 mg/10g
20:4 Arachidonic	<0.0007 g/10g	Methionine	40.1 mg/10g	<b>Niacin by Microbiological Method</b>	
20:5 Eicosapentaenoic	<0.0007 g/10g	<b>Ash</b>		Niacin	1.02 mg/10g
24:0 Lignoceric	0.0030 g/10g	Ash	1.94 g/10g	<b>Pyridoxine</b>	
22:5 Docosapentaenoic	<0.0007 g/10g	<b>Moisture</b>		Pyridoxine	0.149 mg/10g
22:6 Docosahexaenoic	<0.0007 g/10g	Moisture	0.427 g/10g	<b>Folic Acid by Microbiological Method</b>	
Total 18:1 trans	0.0100 g/10g	<b>Iodine by ICP-MS</b>		Folic Acid	89.5 mcg/10g
Total 18:1 cis	0.0161 g/10g	Iodine	3.51 mcg/10g	<b>Vitamin B12 by Microbiological Method</b>	
Total 18:2 trans	0.0185 g/10g	<b>Selenium *</b>		Vitamin B12	0.017 mcg/10g
Total 18:3 trans	0.0389 g/10g	Selenium	0.832 mcg/10g	<b>Biotin by Microbiological Method</b>	
<b>Pantothenic Acid by Microbiological Method</b>		<b>Carotenes</b>		Biotin	1.68 mcg/10g
Pantothenic Acid	0.129 mg/10g	Beta Carotene	4.47 mg/10g		

**Table 3.2: Nutritional components added to miR and purified diets.**

10% Arabidopsis diet		Purified diet	
Ingredient	gram/kg	Ingredient	gram/kg
Aradopsis	100	Casein	200
Sucrose	500	Sucrose	500
Corn starch	130.98	Corn starch	150.48
Corn Oil	40	Cellulose	50
Casein	30	Corn Oil	33.67
Cellulose	28.07	Soybean	7.23
Calcium Phosphate Monobasic	4.73	Safflower	3.95
Tricalcium Phosphate	2.99	Bacon Flavor	5
Mineral mix	13.37	Mineral Mix	13.37
L---Glutamic Acid	26.75	Calcium Carbonate	7.68
L---Proline	14.04	Calcium Phosphate Dibasic	7.03
Vitamin mix	10	Potassium Citrate	5.25
L---Lysine	13.17	Magnesium Oxide	0.79
L---Leucine	10.01	Vitamin Mix	10
L---Cystine	0.23	L-Methionine	3
L---Tyrosine	7.49	Choline Bitartrate	2
L---Methionine	6.43	Ascorbic Acid	0.49
L---Serine	7.27	Beta Carotene	0.045
L---Isoleucine	6.94	Total	1000
L---Valine	8.12		
L---Histidine	3.53		
L---Tryptophan	1.71		
L---Threonine	5.34		
L---Aspartic Acid	6.86		
L---Phenylalanine	5.08		
Bacon Flavor	5		
L---Arginine	4.04		
L---Alanine	2.39		
Glycine	2.21		
L---Glutamine	1.51		
Choline Bitartrate	1.64		
Total	999.9		

**Table 3.3: Final nutritional content of miR and purified diets**

Nutrient	Diet			Nutrient	Diet		
	miR	Purified			miR	Purified	
Alanine	4.6	4.6	gm/kg	Leucine	14.6	14.6	gm/kg
Arginine	6.4	6.4	gm/kg	Lysine	13.0	13.0	gm/kg
Aspartic Acid	11.2	11.2	gm/kg	Magnesium	1.0	1.0	gm/kg
Beta Carotene	44.7	44.7	gm/kg	Manganese	58.5	58.5	mg/kg
Biotin	0.2	0.2	mg/kg	Methionine	7.5	7.5	gm/kg
Boron (Br)	5.0	5.0	gm/kg	Monounsaturated	12.7	13.0	gm/kg
C10:0 Capric	0.0	0.0	gm/kg	Niacin	40.0	40.0	mg/kg
C14:0 Myristic	0.1	0.1	gm/kg	Pantothenic Acid	15.9	14.7	mg/kg
C16:0 Palmitic	6.4	5.9	gm/kg	Ash	3.2	3.4	gm/kg
C16:1 Palmitoleic	0.2	0.2	gm/kg	Carbohydrate	66.3	64.3	gm/kg
C18:0 Stearic	1.7	1.9	gm/kg	Fat	5.1	5.1	gm/kg
C18:1 Oleic	12.2	12.6	gm/kg	Fiber	4.8	4.8	gm/kg
C18:2 Linoleic	22.3	25.3	gm/kg	Phenylalanine	7.8	7.8	gm/kg
C18:3 Linolenic	1.3	1.2	gm/kg	Phosphorus	2.8	2.8	gm/kg
C20:0	0.0	0.0	gm/kg	Polysaccharides	116	133	gm/kg
C20:1	0.1	0.1	gm/kg	Polyunsaturated	23.3	26.0	gm/kg
C22:0	0.0	0.0	gm/kg	Potassium	5.4	5.5	gm/kg
C24:0	0.0	0.0	gm/kg	Protein	18.1	18.1	gm/kg
Calcium	5.2	5.2	gm/kg	Proline	18.0	18.0	gm/kg
CCarbohydrate	2.65	2.57	gm/kg	Pyridoxine	7.3	7.3	mg/kg
CFat	0.46	0.46	gm/kg	Riboflavin	9.0	9.0	mg/kg
Chloride	1.6	1.6	mg/kg	Saturated	8.5	8.2	gm/kg
Cholesterol	1.0	0.1	gm/kg	Selenium	0.2	0.2	mg/kg
Choline	822	822	mg/kg	Serine	10.0	10.0	gm/kg
Chromium	2.0	2.0	gm/kg	Sodium	1101	1019	mg/kg
Copper	6.9	6.0	mg/kg	Sulfur	337	337	mg/kg
CProtein	0.72	0.72	gm/kg	Thiamin	6.1	6.0	mg/kg
CTotal	3.83	3.75	gm/kg	Threonine	7.7	7.7	gm/kg
Cystine	0.5	0.5	gm/kg	Tryptophan	2.0	2.0	gm/kg
Disaccharides	518	510	gm/kg	Tyrosine	10.0	10.0	gm/kg
Folic Acid	2.9	2.0	mg/kg	Valine	11.4	11.4	gm/kg
Fructose	0.2	0.0	gm/kg	Vitamin A	5021	5142	IU/kg
Glucose	0.4	0.0	gm/kg	Vitamin B12	10.0	10.0	mcg/kg
Glutamic Acid	35.6	35.6	gm/kg	Vitamin C	489	489	gm/kg
Glycine	4.3	4.3	gm/kg	Vitamin D3	1000	1000	IU/kg
Histidine	4.8	4.8	gm/kg	Vitamin E	121	110	IU/kg
Iodine	0.2	0.2	mg/kg	Vitamin K1	4.8	4.8	mg/kg
Iron	37.0	37.0	mg/kg	Vitamin K3	1.0	1.0	mg/kg
Isoleucine	9.6	9.6	gm/kg	Zinc	38.1	37.0	mg/kg

## CHAPTER 4

### PLANT EXOSOME-LIKE VESICLES: A POTENTIAL DELIVERY VEHICLE FOR MIRNAS

#### 4.1 INTRODUCTION

##### 4.1.1 ORAL DELIVERY OF MAMMALIAN TUMOR SUPPRESSOR MIRNAS FROM PLANTS IS AN EFFECTIVE CHEMOPREVENTATIVE STRATEGY FOR CRC

In the previous chapter, we established that incorporating lyophilized *Arabidopsis thaliana* bioengineered to express mammalian tumor suppressor miRNAs into a healthy mouse diet is an effective chemopreventive strategy for treating CRC. The tumor burden was nearly two-fold lower in the treated mice compared to those fed a control purified diet (n=6, p=0.045). The dosage of tumor suppressor miRNAs provided in this feeding experiment was approximately 680 ng/day. Though the dosage is far less than the 23 ug/day of synthesized miRNA mice received in our published pilot study, it is consistent with published results showing miRNA in plants via a natural plant diet is delivered nearly 1000 X more efficiently than gavaged synthetic miRNAs (Zhou et al., 2014). As exciting as these results may be, finding alternative ways to administer plant made tumor suppressor miRNAs should be pursued. One reason is it may be impractical to treat humans by comprising 10% of their total daily diet with transgenic lyophilized plant tissue. Another issue is palatability, especially with even higher concentrations of

lyophilized plant material. Thus, our lab sought out a method to increase the amount of plant made mammalian tumor suppressor miRNAs delivered orally while reducing the amount of plant material.

#### 4.1.2 POTENTIAL UPTAKE MECHANISM OF FUNCTIONAL EXOGENOUS PLANT MIRNAS IN MAMMALS

Since the discovery of a cross-kingdom gene regulation pathway between plants and animals, several labs have sought out a possible mechanism that could explain the uptake of these plant miRNAs (Witwer and Hirschi, 2014). One proposed mechanism is that plants package miRNAs into exosome-like vesicles (EVs) that are taken up by the mammalian GI tract after ingestion (Zhang et al., 2016). Plant EVs are much like animal exosomes: they are small lipid vesicles (~100nm) that carry and protect cargo, such as proteins and miRNAs, and deliver them throughout the organism (Record, 2013). Plant EVs have been shown to survive the extreme conditions of the mammalian digestive tract, protecting and delivering their contents to intestinal stem cells and macrophages (Wang et al., 2014). Interestingly, it has been reported that plant EVs can also be delivered to tissues via intravenous, intraperitoneal, and intranasal injections, demonstrating they are highly versatile as a delivery vehicle (Wang et al., 2013). There is also evidence that plant EV membranes act as natural anti-inflammatory agents, in contrast to the toxicity associated with many synthetic delivery methods (Mu et al., 2016).

## 4.2 RESULTS AND DISCUSSION

### 4.2.1 EVS FROM TRANSGENIC PLANTS CONTAIN TUMOR SUPPRESSOR MIRNAS

To determine if EVs could be used to deliver plant-made mammalian tumor suppressor miRNAs, we first examined whether our bioengineered miRNAs were loaded into plant EVs. To isolate EVs from plants we followed a well-established exosome isolation procedure (Zhuang et al., 2015). Fresh tissue from each bioengineered plant line was processed using a commercial juicer, a process that separates out a large portion of plant solids, such as cell walls. The resultant plant juice was then subjected to a series of low-speed centrifuge spins, collecting the supernatant after each spin. The supernatant collected from the last low speed centrifuge spin was pelleted by ultracentrifugation. RNA was isolated from the pellet, which contained the plant EV fraction, and analyzed by RNA gel blot to determine the level of each bioengineered miRNA. Both miR-143 and miR-34a were found at levels comparable to that of an endogenous plant miRNA, miR159a (Figure 4.1). These data demonstrate that plant produced mammalian tumor suppressor miRNAs can be packaged into EVs, thereby providing a potential delivery method for plant-made miRNAs that are packaged in those EVs. However, miR-145 was found at much lower levels in the EV fraction, pointing to

the importance of defining the criteria that control the packaging of miRNAs into these vesicles.

#### 4.2.2 FURTHER PURIFICATION OF CRUDE EV PREP

Though the crude EV preparations contain a high amount of miR-143 and miR-34a, it was desirable to purify the EVs if it could be done without the need for time-consuming and/or expensive additional steps. The pellet formed after ultracentrifugation consists of two visibly different layers: a top layer of a clear waxy substance, and a bottom dark green layer that contained a large amount of plant debris. It was discovered that the two layers could easily separate with gentle pipetting using phosphate buffered saline (PBS), causing the top layer to literally float to the top of the PBS. This floating layer was analyzed by transmission electron microscope (TEM) to verify that the preparation contained EV-like vesicles (Figure 4.2). RNA was isolated from both layers and RNA gel blot analysis was used to show that the upper floating layer contained a higher concentration of miR-143 and miR-34a than the green bottom layer (Figure 4.3). The bottom layer also contained a higher amount of total RNA on average (~200µg) than the top layer (~60µg). This quick and cost-effective method of EV enrichment will be useful in future studies where large quantities of EVs are needed in feeding experiments.

#### 4.2.3 LYOPHILIZATION OF EVS STABILIZED MIRNAS

Lyophilization of whole plant tissues was used to stabilize and deliver plant-made mammalian tumor suppressor miRNAs in the previous feeding experiment,

but it was unknown if the miRNAs in the plant EV fraction would be stabilized by lyophilization. However, lyophilization has often been used to stabilize nanovesicles preparations for long periods of time (Greening et al., 2015). To test the stability of miRNAs packaged into plant EVs, the EV fraction was isolated from *Arabidopsis thaliana* bioengineered to express miR-143. RNA was isolated from a portion of the EV fraction immediately after isolated, and the remaining portion of the EV fraction was lyophilized overnight. After lyophilization, the EV preparation was incubated at room temperature, and RNA isolation performed every two days over the course of six days. We found that miRNAs were stable for at least six days in EVs stored at room temperature after lyophilization (Figure 4.4), raising the possibility that the EV fraction of the lyophilized plant material from the feeding experiment may have been the acting delivery mechanism in the feeding experiment.

#### 4.2.4 ALTERNATIVE CONSTRUCT DESIGNS OF miR-145 TO IMPROVE PACKAGING EFFICIENCY INTO EVS

Our results show that bioengineered miR-143 and miR-34a are packaged into plant exosomes in transgenic plants, but that miR-145 is present in the EV fraction at much lower levels. The majority of plant miRNAs are 21 nt long and start with a 5'U, a characteristic found in both miR-34a and miR-143 (Lee et al., 2015; Laubinger et al., 2008; Bologna et al., 2013). In contrast, miR-145 has neither of these highly conserved traits, as it is 23 nt in length and starts with a 5'G (Figure 4.5A). In plants, small RNAs that are 24 nt long are associated with transcriptional

silencing and are expected to stay in the nucleus (Melnyk et al., 2011). The 5' nucleotide of miRNAs also plays a role in a small RNA's destiny as either a transcriptional or translational silencing small RNA (Chen, 2016). Therefore, several constructs were designed to determine if either the 5' nucleotide or the size of the miRNA plays a role in loading into plant EVs.

To determine if the loading of miR-145 into EVs is determined by the 5' nucleotide, a construct was designed replacing the 5'G with a 5'U (Figure 4.5B). To determine if the loading of miR-145 into EVs is determined by length, a 21nt miR-145 construct was designed by removing two nucleotides from the 3' end (Figure 4.5C). An additional construct was made that was designed to change both of these features: the 5' nucleotide was changed from G to U and two nucleotides were removed from the 3' end. This construct would be used to determine if a combination of these two factors was needed to influence loading into EVs (Figure 4.5D). Cloning of miRNA constructs and generation of transgenic *Arabidopsis thaliana* lines was carried out as previously described in section 2.2.2. Changing the 5' nucleotide and/or removing two nucleotides from the 3' end of miR-145 should have no impact on miRNA functionality, as the seed region (a highly conserved region on miRNAs needed for target recognition in mammals), is located at nucleotides 2-7 from the 5' end of miRNA sequence (Mullany et al., 2016).

#### 4.2.5 THE 5' POSITION DETERMINES LOADING OF miR-145 INTO EVs.

To determine if the modified versions of miR-145 were packaged into the plant EV fraction, EV preparations were prepared for each of transgenic lines expressing those constructs as previously described in section 4.2.2. Using RNA gel blot analysis, the expression levels of each miR-145 version in the EV fraction was determined as compared to the overall level of expression in fresh leaves of the plant (Figure 4.6). The transgenic plant lines all expressed high levels of the miR-145 version they were engineered to produce in the whole plant tissues. However, loading into the plant exosome fraction was greatly enhanced in each of the modified miR-145 versions with a 5'U instead of the natural 5'G. In contrast, loading of the miR-145 versions was unaffected by size. Overall, these results point to a key role of the 5' nucleotide in exosome loading, and are an important first step in defining the characteristics that regulate loading of miRNAs into plant exosomes.

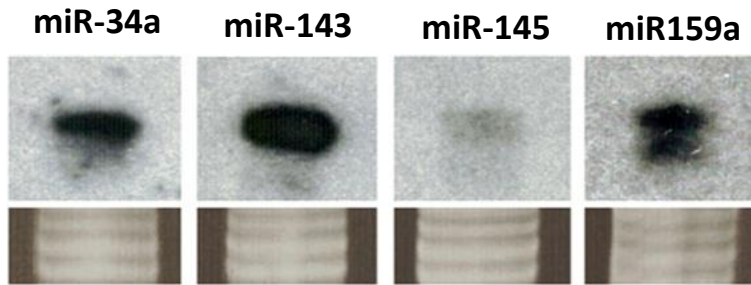


**Figure 4.1: Levels of miRNAs loaded into EVs.** EVs were isolated from a mixture of equal amounts of our three transgenic plant lines. 10  $\mu\text{g}$  of RNA isolated from the exosomes was loaded into each of four lanes of a small RNA gel. The resulting blot was cut to separate the four lanes, and each was hybridized separately for miR-34a, mir-143, miR-145, or the endogenous plant miR159a. The ethidium bromide (EtBr) stained gel is shown as loading control below the autoradiograms.

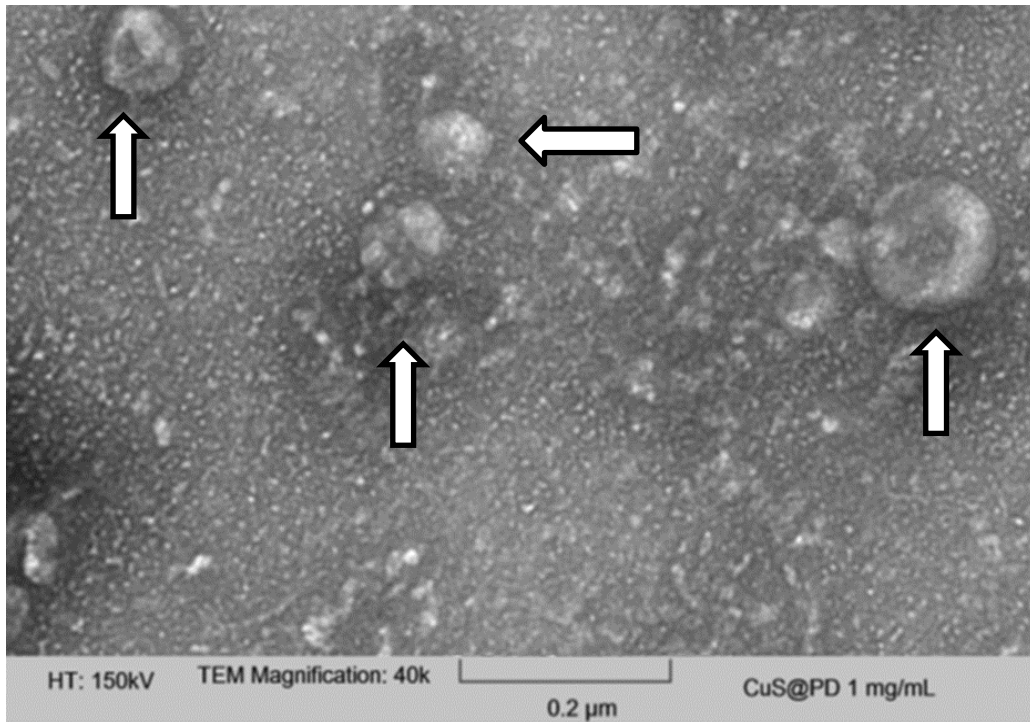


**Figure 4.2: Image of EVs.** A transmission electron microscope (TEM) was used to capture an image of plant EVs after exosome preparation. After EVs were pelleted by ultracentrifugation and resuspended in PBS they were imaged using a TEM. Black arrows indicate EV

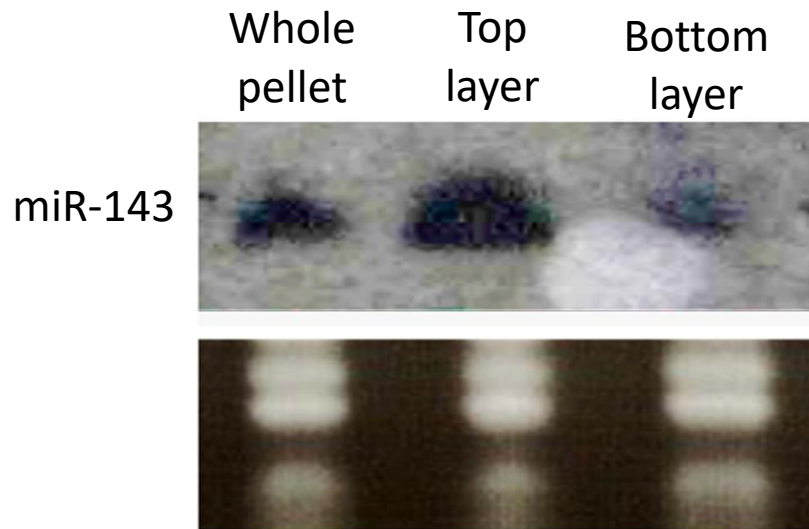


**Figure 4.3: miR-143 localization in floating and non-floating EV prep.** EVs were isolated from a transgenic plant lines expressing miR-143. PBS was used to separate the floating layer from the non-floating layer, these layers were compared to a whole unseparated EV pellet. 10 µg of RNA isolated from each EV fraction were loaded into a small RNA gel. The ethidium bromide (EtBr) stained gel is shown as loading control below the autoradiograms.

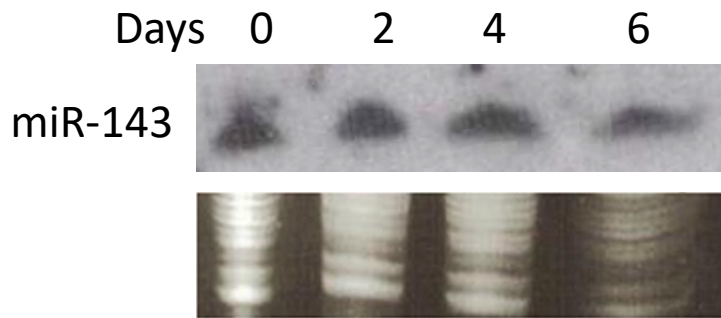


**Figure 4.4: Stability of miR-143 in EVs after lyophilization.** EVs were isolated from a transgenic plant lines expressing miR-143 and resuspended in PBS, with RNA isolated immediately after EV prep. The EV prep was then lyophilized and left at room temperature for 6 days, with RNA being isolated at 2, 4, and 6 days. 10  $\mu$ g of RNA isolated from each EV lyophilization and were loaded into a small RNA gel. The ethidium bromide (EtBr) stained gel is shown as loading control below the autoradiograms.

<b>A</b>	<b>miR-145 23nt - 5'G</b>
	<b>5'- GUCCAGUUU<u>U</u>CCCAGGAAUCCCU-3'</b>
<b>B</b>	<b>miR-145 23nt - 5'U</b>
	<b>5'- <u>U</u>UCCAGUUUCCCAGGAAUCCCU-3'</b>
<b>C</b>	<b>miR-145 21nt - 5'G</b>
	<b>5'- GUCCAGUUUCCCAGGAAUCC <span style="background-color: red; color: black;">■■■</span>-3'</b>
<b>D</b>	<b>miR-145 21nt - 5'U</b>
	<b>5'- <u>U</u>UCCAGUUUCCCAGGAAUCC <span style="background-color: red; color: black;">■■■</span>-3'</b>

**Figure 4.5: Alternative size and starting nucleotide constructs of miR-145.** Constructs changing the size of miR-145 and the 5' nucleotide were designed to determine if they were factors in EV loading. Nucleotides highlighted in yellow have been replaced with a U. Areas highlighted in red are where nucleotides were removed to generate a 21 nt construct **(A)** miR-145 23 nt 5'G **(B)** miR-145 23 nt 5'U **(C)** miR-145 5'G 21 nt **(D)** miR-145 21 nt 5'U

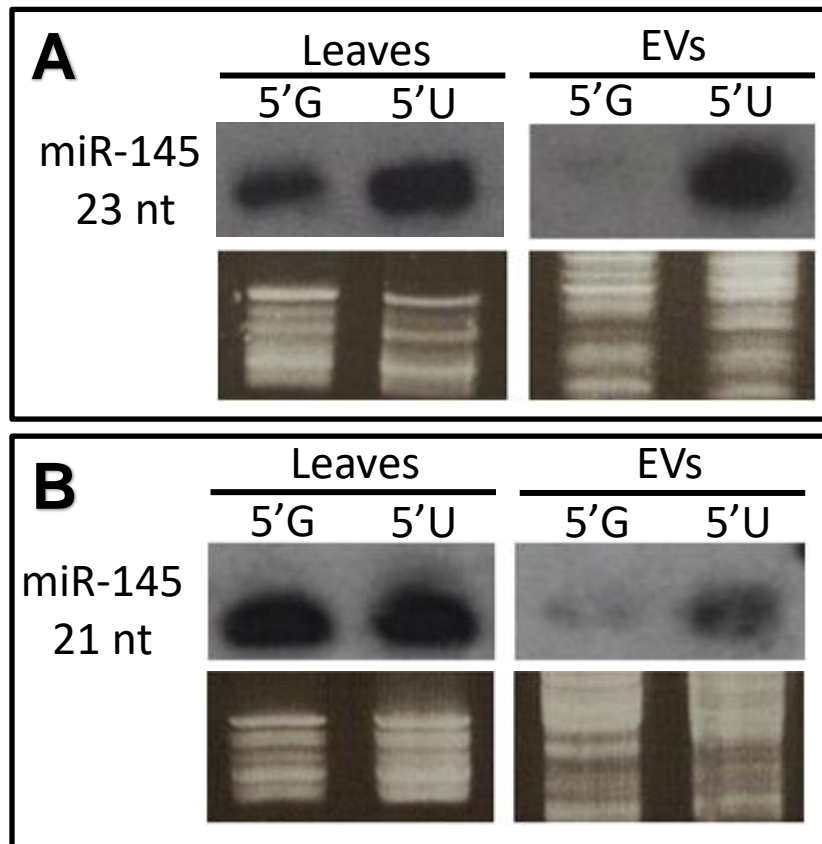


**Figure 4.6: levels of miR-145 constructs loaded into EVs.** EVs were isolated from four transgenic lines plant lines. 10  $\mu$ g of RNA was isolated from fresh *Arabidopsis* tissue and EV preps, then loaded into each of 8 lanes of a small RNA gel. **(A)** Levels of miR-145 23 nt with a 5'G and a 5'U are compared in both fresh *Arabidopsis* and EVs. **(B)** Levels of miR-145 21 nt with a 5'G and a 5'U are compared in both fresh *Arabidopsis* and EVs. The ethidium bromide (EtBr) stained gel is shown as loading control below the autoradiograms.

## CHAPTER 5

### MATERIALS AND METHODS

#### Tumor suppressor miRNA constructs

The tumor suppressor miRNAs inserts were generated using the following gene blocks purchased from Integrated DNA Technologies.

#### miR-34a 21 nt

cacccaaacacacgctcggacgcatattacacatgttcatacacttaatactcgctgtttgaattgatgttttagga  
atatatatgtagCACCCAGCTAAGAGACTGCCTtcacaggctcgtgatatgattcaattagcttccgac  
tcattcatccaaataccgagtcgcaaaaattcaaactagactcgtaaataatgaatgaatgatgcggtagacaaatt  
ggatcattgattctctttgaTGGCAGTGTCTTAGCTGGTTGctctcttttgattccaatttcttgattaat  
cttcctgcacaaaaacatgcttgatccactaagtgacatatatgctgccttcgtatatatagttctggtaaaattaac  
atcttggtttatctttatattaaggcatcgccatg

#### miR-143

cacccaaacacacgctcggacgcatattacacatgttcatacacttaatactcgctgtttgaattgatgttttagga  
atatatatgtagaGAACTACAGTGCTACATCTCTtcacaggctcgtgatatgattcaattagcttccga  
ctcattcatccaaataccgagtcgcaaaaattcaaactagactcgtaaataatgaatgaatgatgcggtagacaaat  
tggatcattgattctctttgaTGAGATGAAGCACTGTAGCTCtctctcttttgattccaatttcttgattaa  
tcttcctgcacaaaaacatgcttgatccactaagtgacatatatgctgccttcgtatatatagttctggtaaaattaa  
catttggtttatctttatattaaggcatcgccatg

miR-145 23 nt 5'G

cacccaaacacacgctcggacgcatattacacatgttcatacacttaataactcgctgtttgaattgatgttttagga  
atatatatgtagaAGGGTCCTGGGAATACTGGAGtcacaggtcgtgatatgattcaattagcttccg  
actcattcatccaaataccgagtcgcaaaaattcaaactagactcggttaaataatgaatgaatgatgcggtagacaa  
attggatcattgattctctttgaGTCCAGTTTTCCCAGGAATCCCTtctctctttgtattccaattttctg  
attaatctttcctgcacaaaaacatgcttgatccactaagtgacatatatgctgccttcgtatatatagttctggtaa  
attaacattttgggtttatctttatthaaggcatcgccatg

miR-145 23 nt 5'U

cacccaaacacacgctcggacgcatattacacatgttcatacacttaataactcgctgtttgaattgatgttttagga  
atatatatgtagaAGGGTCCTGGGAATACTGGAUtcacaggtcgtgatatgattcaattagcttccg  
actcattcatccaaataccgagtcgcaaaaattcaaactagactcggttaaataatgaatgaatgatgcggtagacaa  
attggatcattgattctctttgaUTCCAGTTTTCCCAGGAATCCCTtctctctttgtattccaattttctg  
attaatctttcctgcacaaaaacatgcttgatccactaagtgacatatatgctgccttcgtatatatagttctggtaa  
attaacattttgggtttatctttatthaaggcatcgccatg

miR-145 21 nt 5'G

cacccaaacacacgctcggacgcatattacacatgttcatacacttaataactcgctgtttgaattgatgttttagga  
atatatatgtagGGCTTCCTGGGAATACTGGAGtcacaggtcgtgatatattcaattagcttccgact  
cattcatccaaataccgagtcgcaaaaattcaaactagactcggttaaataatgaatgaatgatgcggtagacaaattg  
gatcattgattctctttgaGTCCAGTTTTCCCAGGAATCCctctctttgtattccaattttctgattaatctt  
tctgcacaaaaacatgcttgatccactaagtgacatatatgctgccttcgtatatatagttctggtaaattaacatt  
ttgggtttatctttatthaaggcatcgccatg

miR-145 21 nt 5'U

cacccaaacacacgctcggacgcatattacacatgttcatacacttaataactcgctgtttgaattgatgttttagga  
atatatatgtagGGCTTCCTGGGAATACTGGATtcacaggctcgatattcaattagcttccgact  
cattcatccaaataccgagtcgccaaaattcaaactagactcgtaaataatgaatgatgacggttagacaaattg  
gatcattgattctctttgaTTCCAGTTTTCCCAGGAATCCctctctttgtattccaatttcttgattaatctt  
tcctgcacaaaaacatgcttgatccactaagtacatatatgctgccttcgtatatatagttctggtaaaattaacatt  
ttgggttatctttatattaaggcatcgccatg

Gene block product was inserted into the pENTR vector using the Invitrogen pENTR Directional Cloning Kit (K2400). These entry vectors were recombined with pSITE-0A destination vector using Gateway LR Clonase Enzyme Mix (Invitrogen, 11791).

#### Generation of transgenic *Arabidopsis thaliana* lines

All *Arabidopsis* plants used to establish transgenic lines were grown at 23°C in long day conditions. All *Arabidopsis* plants were of the Columbia (Col-0) ecotype. *Agrobacterium tumefaciens* strain GV3101 was transformed with pSITE destination vector containing tumor suppressor miRNA constructs and grown overnight at 28°C in 30 mL of LB medium with antibiotics rifampicin, carbenicillin, and kanamycin at concentrations of 50, 100, and 50 g/mL, respectively. The overnight culture was added to 300 mL of fresh medium with the same antibiotics and grown to the stationary phase (OD<sub>600</sub> ~2.0). Cells were harvested by centrifuging at 5500g for 20 min. The pellet was resuspended in infiltration medium

(5% sucrose, 0.05% Silwett L-77) to obtain the desired density (OD600 of 0.8 or >2.0). Plants were inoculated by submersing inflorescences in the bacteria suspension (Clough and Bent, 1998). Saran wrap was then used to provide a high humidity environment and plants were placed in darkness for 10 h. Seeds were collected when all siliques were dry then disinfected with 95% ethanol for 10 min and 0.1% Tween 20 detergent for 15 min and rinsed twice with 100% ethanol. Once dried they were placed in LB with kanamycin (50 g/mL), with 300-400 seeds per Petri dish. Seeds were incubated for approximately 10 d, until plants reached the 4-leaf stage, to ensure kanamycin resistance. Transformants were transplanted into heavily moistened potting soil where plants and grown under long day conditions until seeds set. Seeds were collected, disinfected, and placed on selective LB KAN media again. Transformants from lines expressing resistance at a  $\frac{3}{4}$  ratio were transplanted into heavily moistened potting soil where plants and grown under long day conditions until seeds set. Seeds were collected, disinfected, and placed on selective LB Kan media again. Lines expressing 100% Kan resistance where RNA isolation was performed from whole population, using TRIzol reagent (Life Technologies) as specified in the protocol, to check expression level by RNA gel blot analysis previously described (Mlotshwa et al., 2005).

#### total plant RNA

Total plant RNA was isolated from flash frozen *Arabidopsis thaliana*, using TRIzol reagent (Life Technologies) according to the manufacturer's instructions.

Total plant RNA contains all high and low molecular weight RNA species present in the plant. Therefore, it contains all endogenous plant RNAs, including, for example, mRNAs, tRNAs and rRNA, as well as the entire set of endogenous plant miRNAs. In general, there is no homology between plant and animal miRNAs, although one bioinformatics study indicated that plants and animals share members of the miR854 family (Millar and Waterhouse, 2005; Arteaga-Vazquez et al., 2006; Jones-Rhoades et al., 2006)

#### RNA isolation from mouse tissue

Flash frozen intestinal sections for RNA isolation were stored at -70°C. The frozen tissues were disrupted with a hand-held polytron at maximum speed in the presence of 10 ml of TRIzol reagent (Life Technologies) per gram of tissue, and total RNA was isolated according to manufacturer instructions.

#### RNA gel blots

RNAs (10µg) were resolved on denaturing polyacrylamide gels (20% PAA, 19:1 acrylamide/bis, 7 M urea) in 0.5 × TBE as described (Mlotshwa et al., 2005). The membranes were probed with specific oligodeoxynucleotides (ODNs) complementary to the annotated mouse miRNAs miR-34a ACAACCAGCTAAGACACTGCCA, miR-143 GAGCTACAGTGCTTCATCTCA, miR-145 AGGGATTCCTGGGAAAAGTGGAC, miR159a UUUGGAUUGAAGGGAGCUCUA, miR168a UCGCUUGGUGCAGGUCGGGAA (miRBase). The ODNs were labeled with [ $\gamma$ 32P] ATP (5000 Ci/mmol, Hartmann

Analytics) Specific miRNA probes were prepared by end-labeling antisense oligonucleotides with T4 polynucleotide kinase (New England Biolabs). Pre-hybridizations and hybridizations were carried out under the same conditions at 42°C using Ambion ULTRAhyb oligo hybridization solution. After hybridization, the membranes were washed three times in a low-stringency buffer solution (2 × SSC and 0.1% SDS) for 20 minutes.

#### miRNA next generation sequencing

Libraries were generated using NEBNext Ultra II RNA Library Prep Kit for Illumina (New England Biolabs), and libraries were generated according to manufacturer instructions. Libraries were sent over night on ice to University of Alabama Birmingham, The Heflin Center Genomics Core. Quality control was performed on a HighSensitivity DNA chip on the BioAnalyzer followed by 75bp sequence reads single end read performed on the NextSeq500. Sequencing generated between 15 million and 25 million reads. Sequencing analysis was performed on CLC Genomics Workbench (Qiagen), libraries were analyzed according to manufacturer instructions. High quality reads were annotated to miRbase then normalized to reads per million.

#### mRNA next generation sequencing

Libraries and sequencing was performed on pooled miR and purified diet samples were generated University of Alabama Birmingham, The Heflin Center Genomics Core. They generated the library by subjecting samples to two rounds of polyA

selection followed using the Agilent SureSelect Direction RNA-Seq kit using the manufacturer's protocol. Quality control was performed on a HighSensitivity DNA chip on the BioAnalyzer followed by 75bp sequence reads single end read performed on the NextSeq500. Sequencing generated between 15 million and 25 million reads. Sequencing analysis was performed on CLC Genomics Workbench (Qiagen), libraries were analyzed according to manufacturer instructions. High quality reads were annotated then normalized down to the sample with the lowest number of reads.

#### mouse Strains

C57BL/6J-ApcMin/J mice ( $Apc^{Min/+}$ ) were purchased from Jackson Laboratories (Bar Harbor, ME, USA) but were bred and maintained at the Mouse Core Facility of the Center for Colon Cancer Research at the University of South Carolina (USC), Columbia, SC. All aspects of the animal experiments were conducted in accordance with the guidelines and approval of the USC Institutional Animal Care and Use Committee. The  $Apc^{Min/+}$  mouse model of colon cancer is a genetic model of the disease. These mice are relatively healthy and long lived, in contrast to orthotopic models of colon cancer, which quickly succumb to the disease.  $Apc^{Min/+}$  mice do not start to get sick until about 18 weeks of age, at which point they become anemic. They develop muscle wasting at about 20 weeks of age and typically die when about six months old. Our treatment regimen (see below) ended long before  $Apc^{Min/+}$  mice show any signs of illness.

### Experimental diet protocol

Four-week-old male *Apc<sup>Min/+</sup>* mice were divided into 2 treatment groups of six mice each. The treatment groups corresponded to a diet with either 1) 10% *Arabidopsis thaliana* lines bioengineered to express miR-34a, miR-143, and miR-145 2) purified diet matched nutritionally and calorically. Treatment diets above began when the mice were four weeks old and continued daily for six weeks. This time frame is a standard preventive regimen for experiments using *Apc<sup>Min/+</sup>* mice. No weight loss was observed in any of the mice during the entire 42 days of treatment. Because one of the best signs of toxicity of therapeutic treatments has been loss of weight within 3-5 days of treatment, the absence of weight loss in our animals indicates that our treatments had no obvious toxicity. In addition, the animals did not develop anemia during the experiment, as indicated by normal (as opposed to pale) coloration of extremities, further arguing against toxic side effects. Mice were humanely sacrificed by cervical dislocation after administration of anesthesia using isoflurane by inhalation. The small and large intestines were removed, flushed with phosphate buffered saline, and sliced longitudinally. The small intestine was divided into four equal segments with the colon treated as the fifth segment. Sections for RNA isolation were flash frozen on dry ice, and segments for determination of tumor burden were fixed in 10% formalin and stained with 0.002% methylene blue. Tumors were counted under a dissecting microscope by a single highly experienced investigator, who was blinded to the treatments.

### Plant exosome isolation

Plant juice was collected using the omega brand vert low speed juicing system. Juice collected was subjected to several low speed spins at 5°C. Spins were as follows, 10 minutes at 1,000g, the supernatant was collected and spun for 20 minutes at 3,000g, and finally the supernatant was collected and spun for 40 minutes at 10,000g. The supernatant collected from low speed spins is subjected to an ultracentrifuge spin at 15°C, at 150,000g for 90 minutes. Supernatant is discarded, and the pellet is resuspended with PBS. To separate the top layer of the pellet from the bottom layer PBS was lightly pipetted over the top of the pellet. Exosomes collected and resuspend in PBS is stored at -80°C (Wang et al., 2013).

## REFERENCES

- Akao, Y., Y. Nakagawa, I. Hirata, A. Iio, T. Itoh, K. Kojima, R. Nakashima, Y. Kitade, and T. Naoe. 2010. Role of anti-oncomirs miR-143 and-145 in human colorectal tumors. *Cancer Gene Ther.* 17:398–408. doi:10.1038/cgt.2009.88.
- Arteaga-Vazquez, M., J. Caballero-Perez, and J.-P. Vielle-Calzada. 2006. A Family of MicroRNAs Present in Plants and Animals. *Plant Cell Online.* 18:3355–3369. doi:10.1105/tpc.106.044420.
- Bhandari, A., M. Woodhouse, and S. Gupta. 2017. Colorectal cancer is a leading cause of cancer incidence and mortality among adults younger than 50 years in the USA: A SEER-based analysis with comparison to other young-onset cancers. *J. Investig. Med.* 65:311–315. doi:10.1136/jim-2016-000229.
- Bologna, N.G., A.L. Schapire, and J.F. Palatnik. 2013. Processing of plant microRNA precursors. *Brief. Funct. Genomics.* 12:37–45. doi:10.1093/bfpg/els050.
- Chen, X. 2016. HHS Public Access. 21–44. doi:10.1146/annurev.cellbio.042308.113417.Small.
- Chen, X., X. Guo, H. Zhang, Y. Xiang, J. Chen, Y. Yin, X. Cai, K. Wang, G. Wang, Y. Ba, L. Zhu, J. Wang, R. Yang, Y. Zhang, Z. Ren, K. Zen, J. Zhang, and C.Y. Zhang. 2009. Role of miR-143 targeting KRAS in colorectal tumorigenesis. *Oncogene.* 28:1385–1392. doi:10.1038/onc.2008.474.

- Chin, A.R., M.Y. Fong, G. Somlo, J. Wu, P. Swiderski, X. Wu, and S.E. Wang. 2016. Cross-kingdom inhibition of breast cancer growth by plant miR159. *Cell Res.* 26:1–12. doi:10.1038/cr.2016.13.
- Chou, C.H., N.W. Chang, S. Shrestha, S. Da Hsu, Y.L. Lin, W.H. Lee, C.D. Yang, H.C. Hong, T.Y. Wei, S.J. Tu, T.R. Tsai, S.Y. Ho, T.Y. Jian, H.Y. Wu, P.R. Chen, N.C. Lin, H.T. Huang, T.L. Yang, C.Y. Pai, C.S. Tai, W.L. Chen, C.Y. Huang, C.C. Liu, S.L. Weng, K.W. Liao, W.L. Hsu, and H. Da Huang. 2016. miRTarBase 2016: Updates to the experimentally validated miRNA-target interactions database. *Nucleic Acids Res.* 44:D239–D247. doi:10.1093/nar/gkv1258.
- Clapé, C., V. Fritz, C. Henriquet, F. Apparailly, P.L. Fernandez, F. Iborra, C. Avancès, M. Villalba, S. Culline, and L. Fajas. 2009. miR-143 interferes with ERK5 signaling, and abrogates prostate cancer progression in mice. *PLoS One.* 4:1–8. doi:10.1371/journal.pone.0007542.
- Clough, S.J., and A.F. Bent. 1998. Floral dip: A simplified method for *Agrobacterium*-mediated transformation of *Arabidopsis thaliana*. *Plant J.* 16:735–743. doi:10.1046/j.1365-3113X.1998.00343.x.
- Corpet, D.E., and F. Pierre. 2003. Point : From Animal Models to Prevention of Colon Cancer . Systematic Review of Chemoprevention in Min Mice and Choice of the Model System Point : From Animal Models to Prevention of Colon Cancer . Systematic Review of Chemoprevention in Min Mice and Choi. *Cancer Epidemiol. Biomarkers Prev.* 12:391–400.
- Cui, S.Y., R. Wang, and L.B. Chen. 2014. MicroRNA-145: A potent tumour

suppressor that regulates multiple cellular pathways. *J. Cell. Mol. Med.* 18:1913–1926. doi:10.1111/jcmm.12358.

Davis-Dusenbery, B.N., M.C. Chan, K.E. Reno, A.S. Weisman, M.D. Layne, G. Lagna, and A. Hata. 2011. Down-regulation of Krüppel-like Factor-4 (KLF4) by microRNA-143/145 is critical for modulation of vascular smooth muscle cell phenotype by transforming growth factor- $\beta$  and bone morphogenetic protein 4. *J. Biol. Chem.* 286:28097–28110. doi:10.1074/jbc.M111.236950.

Fedewa, S.A., A.G. Sauer, R.L. Siegel, and A. Jemal. 2015. Prevalence of Major Risk Factors and Use of Screening Tests for Cancer in the United States. *Cancer Epidemiol. Biomarkers Prev.* 24:637–652. doi:10.1158/1055-9965.EPI-15-0134.

Gambari, R., E. Brognara, D.A. Spandidos, and E. Fabbri. 2016. Targeting oncomiRNAs and mimicking tumor suppressor miRNAs: Ev trends in the development of miRNA therapeutic strategies in oncology (Review). *Int. J. Oncol.* 49:5–32. doi:10.3892/ijo.2016.3503.

Garneau, N.L., J. Wilusz, and C.J. Wilusz. 2007. The highways and byways of mRNA decay. *Nat. Rev. Mol. Cell Biol.* 8:113–126. doi:10.1038/nrm2104.

Greening, D.W., D.W. Greening, R. Xu, H. Ji, B.J. Tauro, and R.J. Simpson. 2015. Proteomic Profiling. 1295.

Grimson, A., K.K.H. Farh, W.K. Johnston, P. Garrett-Engele, L.P. Lim, and D.P. Bartel. 2007. MicroRNA Targeting Specificity in Mammals: Determinants beyond Seed Pairing. *Mol. Cell.* 27:91–105. doi:10.1016/j.molcel.2007.06.017.

- Haggar, F. a, and R. Boushey. 2009. Colorectal Cancer Epidemiology : Incidence , Mortality , Survival , and Risk Factors. *Clin. Colon Rectal Surg.* 6:191–197. doi:10.1055/s-0029-1242458.
- Hirschi, K.D., G.J. Pruss, and V. Vance. 2015. Dietary delivery: A new avenue for microRNA therapeutics? *Trends Biotechnol.* 33:431–432. doi:10.1016/j.tibtech.2015.06.003.
- Jin, D.J., Y.T. Fang, Z.G. Li, Z. Chen, and J. Bin Xiang. 2015. Epithelial-mesenchymal transition-associated microRNAs in colorectal cancer and drug-targeted therapies (Review). *Oncol. Rep.* 33:515–525. doi:10.3892/or.2014.3638.
- Jones-Rhoades, M.W., D.P. Bartel, and B. Bartel. 2006. MicroRNAs and their regulatory roles in plants. *Annu. Rev. Plant Biol.* 57:19–53. doi:10.1146/annurev.arplant.57.032905.105218.
- Kano, M., N. Seki, N. Kikkawa, L. Fujimura, I. Hoshino, Y. Akutsu, T. Chiyomaru, H. Enokida, M. Nakagawa, and H. Matsubara. 2010. MiR-145, miR-133a and miR-133b: Tumor-suppressive miRNAs target FSCN1 in esophageal squamous cell carcinoma. *Int. J. Cancer.* 127:2804–2814. doi:10.1002/ijc.25284.
- Kent, O.A., M.N. McCall, T.C. Cornish, and M.K. Halushka. 2014. Lessons from miR-143/145: The importance of cell-type localization of miRNAs. *Nucleic Acids Res.* 42:7528–7538. doi:10.1093/nar/gku461.
- Laubinger, S., T. Sachsenberg, G. Zeller, W. Busch, J.U. Lohmann, G. Rättsch, and D. Weigel. 2008. Dual roles of the nuclear cap-binding complex and

- SERRATE in pre-mRNA splicing and microRNA processing in *Arabidopsis thaliana*. *Proc. Natl. Acad. Sci. U. S. A.* 105:8795–800. doi:10.1073/pnas.0802493105.
- Lee, W.C., S.H. Lu, M.H. Lu, C.J. Yang, S.H. Wu, and H.M. Chen. 2015. Asymmetric bulges and mismatches determine 20-nt microRNA formation in plants. *RNA Biol.* 12:1054–1066. doi:10.1080/15476286.2015.1079682.
- Lewis, B.P., C.B. Burge, and D.P. Bartel. 2005. Conserved seed pairing, often flanked by adenosines, indicates that thousands of human genes are microRNA targets. *Cell.* 120:15–20. doi:10.1016/j.cell.2004.12.035.
- Liang, G., H. He, Y. Li, and D. Yu. 2012. A new strategy for construction of artificial miRNA vectors in *Arabidopsis*. *Planta.* 235:1421–1429. doi:10.1007/s00425-012-1610-5.
- Manuscript, A., and E. Dysfunction. 2015. NIH Public Access. 25:713–724. doi:10.1097/MCA.000000000000178.Endothelial.
- Martinez-Trujillo, M., V. Limones-Briones, J.L. Cabrera-Ponce, and L. Herrera-Estrella. 2004. Improving transformation efficiency of *Arabidopsis thaliana* by modifying the floral dip method. *Plant Mol. Biol. Report.* 22:63–70. doi:10.1007/BF02773350.
- Melnyk, C.W., A. Molnar, A. Bassett, and D.C. Baulcombe. 2011. Mobile 24 nt small RNAs direct transcriptional gene silencing in the root meristems of *Arabidopsis thaliana*. *Curr. Biol.* 21:1678–1683. doi:10.1016/j.cub.2011.08.065.
- Millar, A.A., and P.M. Waterhouse. 2005. Plant and animal microRNAs: Similarities

and differences. *Funct. Integr. Genomics*. 5:129–135. doi:10.1007/s10142-005-0145-2.

Mlotshwa, S., G.J. Pruss, J.L. MacArthur, M.W. Endres, C. Davis, L.J. Hofseth, M.M. Peña, and V. Vance. 2015. A novel chemopreventive strategy based on therapeutic microRNAs produced in plants. *Cell Res.* 25:521–4. doi:10.1038/cr.2015.25.

Mlotshwa, S., S.E. Schauer, T.H. Smith, A.C. Mallory, J.M. Herr, B. Roth, D.S. Merchant, A. Ray, L.H. Bowman, and V.B. Vance. 2005. Ectopic DICER-LIKE1 expression in P1/HC-Pro Arabidopsis rescues phenotypic anomalies but not defects in microRNA and silencing pathways. *Plant Cell*. 17:2873–85. doi:10.1105/tpc.105.036608.

Mu, J., X. Zhuang, Q. Wang, H. Jiang, Z. Deng, L. Zhang, S. Kakar, Y. Jun, D. Miller, and H. Zhang. 2016. Interspecies communication between plant and mouse gut host cells through edible plant derived exosome-like nanoparticles. 58:1561–1573. doi:10.1002/mnfr.201300729.Interspecies.

Mullany, L.E., J.S. Herrick, R.K. Wolff, and M.L. Slattery. 2016. MicroRNA Seed Region Length Impact on Target Messenger RNA Expression and Survival in Colorectal Cancer. *PLoS One*. 11:e0154177. doi:10.1371/journal.pone.0154177.

Nalls, D., S.N. Tang, M. Rodova, R.K. Srivastava, and S. Shankar. 2011. Targeting epigenetic regulation of mir-34a for treatment of pancreatic cancer by inhibition of pancreatic cancer stem cells. *PLoS One*. 6. doi:10.1371/journal.pone.0024099.

- Pagliuca, a, C. Valvo, E. Fabrizi, S. di Martino, M. Biffoni, D. Runci, S. Forte, R. De Maria, and L. Ricci-Vitiani. 2013. Analysis of the combined action of miR-143 and miR-145 on oncogenic pathways in colorectal cancer cells reveals a coordinate program of gene repression. *Oncogene*. 32:4806–13. doi:10.1038/onc.2012.495.
- Pastrello, C., M. Tsay, M. Abovsky, E. Pasini, E. Shirdel, M. Angeli, T. Tokar, J. Jamnik, M. Kotlyar, A. Juriscova, J. Kostopoulos, A. El-Sohemy, and I. Jurisica. 2016. Circulating plant miRNAs can regulate human gene expression in vitro. *Sci. reports (In Press)*. 1–9. doi:10.1038/srep32773.
- Perkins, S., R.D. Verschoyle, K. Hill, S. Perkins, R.D. Verschoyle, K. Hill, I. Parveen, M.D. Threadgill, R.A. Sharma, M.L. Williams, W.P. Steward, and A.J. Gescher. 2002. Chemopreventive Efficacy and Pharmacokinetics of Curcumin in the Min / + Mouse , a Model of Familial Adenomatous Polyposis Chemopreventive Efficacy and Pharmacokinetics of Curcumin in the Min / 2 Mouse , a Model of Familial Adenomatous Polyposis 1. 11:535–540.
- Pirf, S., L. Zanella, M. Kenzo, C. Montesano, A. Minutolo, M. Potesta, M.S. Sobze, A. Canini, M. Cirilli, R. Muleo, V. Colizzi, and A. Galgani. 2016. MicroRNA from moringa oleifera: Identification by high throughput sequencing and their potential contribution to plant medicinal value. *PLoS One*. 11:1–25. doi:10.1371/journal.pone.0149495.
- Pramanik, D., N.R. Campbell, C. Karikari, R. Chivukula, O. a Kent, J.T. Mendell, and A. Maitra. 2011. Restitution of tumor suppressor microRNAs using a systemic nanovector inhibits pancreatic cancer growth in mice. *Mol. Cancer*

*Ther.* 10:1470–80. doi:10.1158/1535-7163.MCT-11-0152.

Qian, X., J. Yu, Y. Yin, J. He, L. Wang, Q. Li, L.Q. Zhang, C.Y. Li, Z.M. Shi, Q. Xu, W. Li, L.H. Lai, L.Z. Liu, and B.H. Jiang. 2013. MicroRNA-143 inhibits tumor growth and angiogenesis and sensitizes chemosensitivity to oxaliplatin in colorectal cancers. *Cell Cycle*. 12:1385–1394. doi:10.4161/cc.24477.

Raabe, C.A., T.-H. Tang, J. Brosius, and T.S. Rozhdestvensky. 2014. Biases in small RNA deep sequencing data. *Nucleic Acids Res.* 42:1414–1426. doi:10.1093/nar/gkt1021.

Record, M. 2013. Exosome-like nanoparticles from food: Protective nanoshuttles for bioactive cargo. *Mol. Ther.* 21:1294–1296. doi:10.1038/mt.2013.130.

Saito, Y., T. Nakaoka, and H. Saito. 2015. microRNA-34a as a Therapeutic Agent against Human Cancer. *J. Clin. Med.* 4:1951–1959. doi:10.3390/jcm4111951.

Siegel, R.L., K.D. Miller, and A. Jemal. 2018. Cancer statistics, 2018. *CA. Cancer J. Clin.* 68:7–30. doi:10.3322/caac.21442.

Slabáková, E., Z. Culig, J. Remšík, and K. Souček. 2017. Alternative mechanisms of MIR-34a regulation in cancer. *Cell Death Dis.* 8:1–10. doi:10.1038/cddis.2017.495.

Song, L., M.J. Axtell, and N. V. Fedoroff. 2010. RNA Secondary Structural Determinants of miRNA Precursor Processing in Arabidopsis. *Curr. Biol.* 20:37–41. doi:10.1016/j.cub.2009.10.076.

Takaoka, Y., Y. Shimizu, H. Hasegawa, Y. Ouchi, S. Qiao, M. Nagahara, M. Ichihara, J.D. Lee, K. Adachi, M. Hamaguchi, and T. Iwamoto. 2012. Forced expression of miR-143 represses ERK5/c-Myc and p68/p72 signaling in

concert with miR-145 in gut tumors of Apcmin mice. *PLoS One*. 7. doi:10.1371/journal.pone.0042137.

Wang, B., X. Zhuang, Z. Deng, H. Jiang, J. Mu, Q. Wang, X. Xiang, H. Guo, L. Zhang, G. Dryden, J. Yan, D. Miller, and H. Zhang. 2014. Targeted Drug Delivery to Intestinal Macrophages by Bioactive Nanovesicles Released from Grapefruit. 22:522–534. doi:10.1038/mt.2013.190.

Wang, G., L. Jacquet, E. Karamariti, and Q. Xu. 2015. Origin and differentiation of vascular smooth muscle cells. *J. Physiol.* 593:3013–3030. doi:10.1113/JP270033.

Wang, Q., X. Zhuang, J. Mu, Z. Deng, H. Jiang, L. Zhang, X. Xiang, B. Wang, J. Yan, D. Miller, and H. Zhang. 2013. Delivery of therapeutic agents by nanoparticles made of grapefruit-derived lipids. doi:10.1038/ncomms2886.

Weng, W., J. Feng, H. Qin, Y. Ma, and A. Goel. 2015. An update on miRNAs as biological and clinical determinants in colorectal cancer: a bench-to-bedside approach. *Future Oncol.* 11:1791–808. doi:10.2217/fon.15.83.

Werner, S., H. Wollmann, K. Schneeberger, and D. Weigel. 2010. Structure Determinants for Accurate Processing of miR172a in *Arabidopsis thaliana*. *Curr. Biol.* 20:42–48. doi:10.1016/j.cub.2009.10.073.

Witwer, K.W., and K.D. Hirschi. 2014. Transfer and functional consequences of dietary microRNAs in vertebrates: Concepts in search of corroboration. *BioEssays*. 36:394–406. doi:10.1002/bies.201300150.

Xu, B., J. Cao, J. Zhang, S. Jia, S. Wu, K. Mo, G. Wei, L. Liang, X. Miao, A. Bekker, and Y.-X. Tao. 2017. Role of MicroRNA-143 in Nerve Injury-Induced

Upregulation of Dnmt3a Expression in Primary Sensory Neurons. *Front. Mol. Neurosci.* 10:1–13. doi:10.3389/fnmol.2017.00350.

Yan, X., X. Chen, H. Liang, T. Deng, W. Chen, S. Zhang, M. Liu, X. Gao, Y. Liu, C. Zhao, X. Wang, N. Wang, J. Li, R. Liu, K. Zen, C.Y. Zhang, B. Liu, and Y. Ba. 2014. MiR-143 and miR-145 synergistically regulate ERBB3 to suppress cell proliferation and invasion in breast cancer. *Mol. Cancer.* 13:1–14. doi:10.1186/1476-4598-13-220.

Yang, J., L.M. Farmer, A.A.A. Agyekum, and K.D. Hirschi. 2015. Detection of dietary plant-based small RNAs in animals. *Cell Res.* 25:517–20. doi:10.1038/cr.2015.26.

Yang, J., T. Hotz, L. Broadnax, M. Yarmarkovich, I. Elbaz-Younes, K.D. Hirschi, Z. Zhou, L. Zhang, S. Mlotshwa, K.D. Hirschi, G.J. Pruss, V. Vance, J.W. Snow, A.E. Hale, S.K. Isaacs, A.L. Baggish, S.Y. Chan, K.W. Witwer, M.A. McAlexander, S.E. Queen, R.J. Adams, B. Dickinson, J. Yang, L.M. Farmer, A.A.A. Agyekum, K.D. Hirschi, J. Yang, L.M. Farmer, A.A.A. Agyekum, I. Elbaz-Younes, K.D. Hirschi, J. Yang, K.D. Hirschi, L.M. Farmer, A. Etheridge, C.P. Gomes, R.W. Pereira, D. Galas, K. Wang, H. Valadi, A. Zampetaki, P. Willeit, I. Drozdov, S. Kiechl, M. Mayr, J.D. Arroyo, S. Ju, J. Mu, M. Minekus, S.R. Baier, C. Nguyen, F. Xie, J.R. Wood, J. Zempleni, J. Zempleni, S.R. Baier, K.D. Hirschi, A. Philip, V.A. Ferro, R.J. Tate, K.W. Witwer, K.D. Hirschi, X. Chen, and Y. Wang. 2016. Anomalous uptake and circulatory characteristics of the plant-based small RNA MIR2911. *Sci. Rep.* 6:26834. doi:10.1038/srep26834.

- Zauber, A.G. 2015. The Impact of Screening on Colorectal Cancer Mortality and Incidence: Has It Really Made a Difference? *Dig. Dis. Sci.* 60:681–691. doi:10.1007/s10620-015-3600-5.
- Zhang, L., D. Hou, X. Chen, D. Li, L. Zhu, Y. Zhang, J. Li, Z. Bian, X. Liang, X. Cai, Y. Yin, C. Wang, T. Zhang, D. Zhu, D. Zhang, J. Xu, Q. Chen, Y. Ba, J. Liu, Q. Wang, J. Chen, J. Wang, M. Wang, Q. Zhang, J. Zhang, K. Zen, and C.-Y. Zhang. 2012. Exogenous plant MIR168a specifically targets mammalian LDLRAP1: evidence of cross-kingdom regulation by microRNA. *Cell Res.* 22:107–26. doi:10.1038/cr.2011.158.
- Zhang, M., E. Viennois, C. Xu, and D. Merlin. 2016. Plant derived edible nanoparticles as a new therapeutic approach against diseases. *Tissue Barriers.* 4:1–9. doi:10.1080/21688370.2015.1134415.
- Zhang, X., S. Liu, T. Hu, S. Liu, Y. He, and S. Sun. 2009. Up-regulated microRNA-143 transcribed by nuclear factor kappa B enhances hepatocarcinoma metastasis by repressing fibronectin expression. *Hepatology.* 50:490–499. doi:10.1002/hep.23008.
- Zhou, Z., X. Li, J. Liu, L. Dong, Q. Chen, J. Liu, H. Kong, Q. Zhang, X. Qi, D. Hou, L. Zhang, G. Zhang, Y. Liu, Y. Zhang, J. Li, J. Wang, X. Chen, H. Wang, J. Zhang, H. Chen, K. Zen, and C.-Y. Zhang. 2014. Honeysuckle-encoded atypical microRNA2911 directly targets influenza A viruses. *Cell Res.* 25:39–49. doi:10.1038/cr.2014.130.

Zhuang, X., Z. Deng, J. Mu, L. Zhang, J. Yan, D. Miller, W. Feng, C.J. McClain, and H. Zhang. 2015. Ginger-derived nanoparticles protect against alcohol-induced liver damage. 1:1–18.